Article

Numerical Study of Integrating Thermal Insulation Local Bio-Sourced Materials into Walls and Roofs for Thermal Comfort Improvement in Buildings in a Tropical Climate

Kokou Dowou [1], Yawovi Nougbléga [1,2,*], Kokou Aménuvéla Toka [1] and Komi Apélété Amou [2,3]

[1] Laboratoire Sur l'Energie Solaire/Groupe Phénomène de Transfert et Energétique, Université de Lomé, Lome 01 BP 1515, Togo; kokoudowou1@gmail.com (K.D.); tokakokou@gmail.com (K.A.T.)

[2] Regional Centre of Excellence on Electricity Management (CERME), University of Lomé, Lome 01 BP 1515, Togo; makpamou@yahoo.fr

[3] Laboratoire Sur l'Energie Solaire, Département de Physique, Faculté Des Sciences (FDS), Université de Lomé, Lome 01 BP 1515, Togo

* Correspondence: nycogl@yahoo.fr

Abstract: Thermal insulation is a reliable strategy for achieving optimal thermal comfort in built environments and is among the most effective energy-saving measures. Currently, environmentally friendly insulation materials produced from plant and animal fibers constitute a significant component of the building industry, largely due to their minimal embodied energy and concerns about certain synthetic insulation materials' potential adverse health effects. The main objective of the present study is to encourage and facilitate the utilization of environmentally friendly thermal insulation materials derived from biological sources, including vegetal and animal fibers, to improve thermal comfort and consequently reduce energy consumption in buildings. The study attempts to simulate the indoor air temperature profiles of a single building constructed using locally sourced materials and insulated in a series of stages with the aforementioned insulation materials. Firstly, insulation is applied exclusively to the roof. Secondly, the insulation is applied to the remaining wall surfaces. Alternatively, the insulation is applied to both the roof and the wall surfaces simultaneously. The objective is to ascertain the optimal combination of bio- and geo-insulating materials to achieve thermal comfort in buildings constructed with local materials in tropical climates. The Gauss-Seidel iterative method was employed to solve the energy equations that had been written on the walls and roof of the building. The equations were then discretized using the nodal method. To ascertain the thermal comfort of the simulated buildings, a comparison was made of the indoor air temperatures. The results of the simulations demonstrated that the utilization of wood fiber, reed panels, and straw bales as insulation materials led to a notable enhancement in comfort levels across all five building types, with an average increase of 17.5%. Among these materials, wood fiber emerged as the most effective insulation option, reducing temperatures by up to 19%. Its integration into the sheet metal-clad Banco building would be particularly advantageous. The findings demonstrate that the simultaneous insulation of walls and roofs with natural fiber thermal insulation materials markedly reduces indoor air and wall temperatures in buildings by up to 19% in comparison to uninsulated walls and roofs.

Keywords: numerical simulation; thermal comfort; local building materials; thermal insulation

1. Introduction

The building sector is one of the three largest consumers of energy worldwide, along with the transport and industrial sectors [1,2]. Accounting for nearly 40% of global energy consumption, the building sector is responsible for approximately half of all energy used annually. Of this, a significant proportion is attributable to cooling and heating, which contribute to elevated global greenhouse gas emissions [3,4]. Improved energy efficiency in buildings is an essential element of the strategy to reduce both energy consumption and greenhouse gas emissions in the construction field [5]. Among the most effective and pervasive methods for attaining this objective is the implementation of suitable thermal insulation within the building envelope [6,7].

Utilizing low-thermal-conductivity materials is the fundamental objective of such strategies, which simultaneously aspire to reduce energy expenditure while ensuring the thermal comfort of occupants [8,9]. In the last two decades, natural fibers from cultivated and wild agricultural plants, the wood-processing industry, animal wool, etc., have attracted considerable attention as alternatives for thermal insulation applications due to their widespread availability, sustainability, and cost-effectiveness [8–10].

Fibrous materials are among the most commonly used for thermal and acoustic insulation of building envelopes and are suitable for several applications. In the construction sector, there is an increasing demand for insulation products with a lower environmental impact than traditional insulators such as glass fiber, rock wool, expanded polystyrene, and polyurethane foam [11,12].

Utilizing thermal insulation materials derived from renewable resources constitutes a substitute for those derived from petroleum-based resources. These materials offer many advantages, including biodegradability, low thermal conductivity, sufficient acoustic properties, and low-resource production techniques [13].

The commercial viability of bio-based insulation materials is significant, offering substantial economic benefits. They provide an effective waste management strategy and contribute to environmental sustainability. France has already implemented a commercialization strategy for bio-based insulation materials to minimize operational energy consumption in the building sector. Energy recovery in 2050 is estimated to save 4.1 million m^3 of land, 75,000 tons of fossil fuel, and EUR 89 million [14].

Bio-based insulation materials have a huge market and can be commercialized for better economic benefits. These bio-based insulation materials offer a very efficient waste management strategy and are environmentally friendly. The commercialization of bio-based insulation materials which minimize operational energy consumption in the building sector has already been implemented in France, and it is estimated that, by 2050, the associated energy savings will facilitate the recovery of 4.1 million m^3 of land, 75,000 tons of fossil fuel and 89 million euros [14].

Several studies have examined the effect of insulation on energy consumption in the building sector. For example, Eddiab et al. [15] optimized the insulation thickness of a residential property in Marrakesh, Morocco. The results demonstrated that the 8 cm wood fiber insulation saved 7% of the heat load and 14% of the cold load compared to the 4 cm insulation. In their study, Zhang et al. [16] employed DeST software to simulate the energy consumption of a university building in Chengdu and analyze the impact of material type and exterior wall insulation thickness on this consumption. The findings indicated that incorporating insulation into the exterior walls resulted in a 3.78% reduction in the overall load and a 25.34% decline in the total cost per unit area compared to a scenario with no insulation.

In a study conducted by Kaddouri et al., a series of numerical simulations were carried out using TRNSYS software to assess the impact of applying three bio-based insulation

materials, namely hemp wool, wood fiber, and expanded cork, in the wall layer of the building. Different insulation scenarios were studied to make a choice that would ensure optimum comfort in the building while keeping the energy demand low. The results of this study show that insulating the roof with 8 cm of hemp wool contributes to energy savings of up to 36.7% and 35.2% for cooling and heating demand, respectively [17].

It has been demonstrated that the insulation of walls and roofs can result in energy savings of up to 77% [18,19]. Presently, researchers are seeking to supplant mineral-based insulation with plant materials, given their accessibility and minimal environmental impact. Due to bio-based thermal insulation solutions' potential to improve both the thermal and environmental performance of buildings, Cosentino and al. carried out a study that aims to investigate and compare the functional and ecological characteristics of bio-based materials through an extensive literature review. This review concludes that bio-based insulation materials have significant potential to improve building performance, fulfill requirements, and promote a more sustainable industry. However, further work is still needed to achieve this outcome [20].

Natural fiber insulation materials are more durable when handled. Natural fiber-based insulation materials can be a healthier alternative for insulating contemporary building types such as passive houses, green buildings, and low-energy homes. Natural fiber insulation refers to a range of insulation materials made from natural materials such as cellulose, wool, wood fiber, hemp, flax, and cotton [21]. A study by Dombayci [22] concentrated on the environmental effect of utilizing the optimal insulation thickness, and the findings indicated a reduction of almost 42% in carbon emissions and a 47% decrease in energy consumption. In a related study, Kaynakli [23] investigated the influence of fuel sources on the insulation's optimal thickness. The results demonstrated that the optimal thickness exhibited a range of 5.3–12.4 cm, contingent on the specific fuel type under consideration. Similar findings have been documented by Fokaides and Papadopoulos [24] concerning the climate of the Eastern Mediterranean region. In another study, Özel and Pihtili [25] concentrated on the location and optimal distribution of the insulation layer in the wall at varying orientations.

The research carried out by Nandapala et al. [26] demonstrated that the insulation system on a roof slab can attain a heat gain reduction of over 75%, while concurrently enhancing thermal performance when juxtaposed with alternative solutions, such as a tiled roof. In a further study, Samuel et al. [27] demonstrated that using filler materials within roof structures and incorporating air cavities within wall constructions (a technique known as 'rat trap bonding') can significantly reduce heat transfer through these structures. Implementation of insulation measures within building structures serves to diminish heat transfer, thereby enhancing occupants' comfort and concurrently reducing the burden of energy expenditure [28].

In tropical climates, the optimal construction method for dwelling uses wall panels comprising a combination of natural insulation materials and conventional wall-building components [29]. Marin-Calvo et al. [30] developed an insulating material based on cellulose and rice husks, derived from agro-industrial waste, offering a thermal conductivity of 0.04 W/m·K and good mechanical strength. They proposed utilizing this sustainable material as an alternative for constructing eco-friendly buildings for carbon footprint reduction.

In their study on the energy efficiency of office buildings in Burkina Faso, Zouré et al. [31] tested several insulating materials, including those based on bio-resources and recycled materials. The results of the simulations indicate that hemp wool is the optimal insulating material for walls, roofs, and interior floors, with a potential reduction in annual energy consumption of between 17.7% and 25.8%. This would also contribute to promoting a circular economy in the construction industry. In their study on the impact of local roof

insulation materials on the energy consumption of an earth-straw house, Togueni et al. [32] observed that this type of wall exhibited a reduction in energy consumption of 8% relative to a standard clay wall.

Plant fibers are organic, promising green materials for thermal insulation. They are excellent insulators for heat, obtained from renewable resources, and are biodegradable and eco-friendly. According to a study by Asim et al. [33], lightweight concrete reinforced with natural fibers is an excellent candidate for cladding bricks in building walls. It holds significant promise for improving the thermal insulation of buildings, thereby reducing heating and cooling costs. A study conducted by Asim et al. [33] revealed that coconut and basalt fiber samples demonstrated the highest improvements in thermal insulation, ranging from 6.5% to 17.4% and 5.8% to 17.1%, respectively, as the fiber content increased from 2.5% to 10%. Thermal conductivity typically decreases linearly with an increase in the percentage of natural fibers. Natural fibers offer numerous advantages, including widespread availability, low cost and density, non-toxicity, renewability, and satisfactory mechanical properties.

The utilization of natural insulation materials, such as wool, wheat, and straw, offers the advantage of being eco-friendly and recyclable, unlike traditional insulation materials, which contribute significantly to environmental pollution. According to Chuen's [34] study, straw bales offer satisfactory thermal insulation. However, a thicker layer is needed compared to conventional insulation materials such as mineral wool, EPS, or XPS, due to the slightly higher thermal conductivity of straw bales. Omer et al. [35] demonstrated that coconut fiber is an ideal insulating material for house ceiling boards due to its low thermal conductivity of 0.225 W/m·K and density of 74.23 kg/m^3. The study showed that a ceiling made from coconut fiber with only 10 mm thickness could effectively reduce the amount of heat entering the house by 0.225 W. Additionally, coconut fiber's ability to reduce heat makes it a viable solution for wall coverings to block solar heat radiation from the outside [36].

A study conducted by Malheiro [37] showed that reed has characteristics that make it suitable for use as a building material, particularly as a thermal insulation material. Additionally, given the abundance of reeds, it presents a sustainable, eco-friendly, and low-cost option. Sakthivel et al. [38] evaluated six types of recycled cotton mats, which were produced and tested to determine their thermal insulation and acoustic absorption properties. The authors observed that cotton mats provide the best thermal insulation and acoustic absorption.

A substantial corpus of literature exists on the subject of thermal insulation. It has been extensively studied from different perspectives, and considerable success has been achieved in terms of its application to the building envelope to reduce energy consumption and associated emissions [39–41]. This research aims to propose and develop bio-sourced insulation solutions for the insulation of domestic building envelopes, intending to improve the thermal comfort of energy-efficient buildings constructed using locally sourced eco-building materials in tropical climate zones.

A review of the current literature indicates a notable absence of research exploring the integration of thermal insulation for roofs and building walls with bio-sourced materials. The authors of this article propose a study to examine the integration of thermal insulation for roof walls and building walls in hot tropical climates. This study has undertaken a significant research challenge: to achieve thermal comfort and thermal efficiency for the construction systems under investigation. The study's originality lies in its utilization of plant fibers for the coupled insulation of walls and roofs, intending to enhance thermal comfort. This subject is currently underrepresented in the literature.

To this end, a numerical model has been developed to predict heat transfer for a series of energy-efficient construction systems. This study also includes a comparative analysis of thermal profiles for indoor air and housing walls.

2. Materials and Methods

2.1. Raw Materials

This research used a combination of five different types of buildings and five natural fiber thermal insulators (wood fiber, straw bales, reed panels, coconut fiber, and cotton wool) to explore the thermal properties of the materials used to construct the buildings, as well as the compositions of the thermal insulation materials. The results are presented in the following tables. Tables 1 and 2 present a comprehensive listing of the thermal properties of environmentally friendly thermal insulation materials and the material composition of the constructive elements utilized in the insulation process.

Table 1. Thermal properties of thermal insulating materials used [42,43].

Insulation Materials	Thermal Conductivity λ ($\text{W·m}^{-1}\text{·K}^{-1}$)	Density ρ (Kg·m^{-3})	Heat Capacity C_p ($\text{J·Kg}^{-1}\text{·K}^{-1}$)	Thickness d (cm)	Thermal Resistance R ($\text{m}^2\text{K·W}^{-1}$)
Coconut fibers	0.047–0.07	20–50	1500–1800	10	1709
Cottonwood	0.040	25–30	1600	10	2500
Straw bale	0.045–0.07	70–120	1400–2000	10	1739
Reed panels	0.055–0.09	120–255	1400–2000	10	1379
Wood wool	0.050	110–160	1600–2300	10	2000

Table 2. Composition of materials utilized in the construction of insulating elements.

Types of Habitat (Walls and Roof)	Types of Insulation	Insulating Materials with 10 cm Thickness
Breezeblock + Concrete slab	Internal roof insulation External wall insulation Internal roof insulation and external wall insulation	Coconut fibers, cotton wool, straw bale, reed panels, wood fibers
Stone + Sheet metal (wavy)		Coconut fibers, cotton wool, straw bale, reed panels, wood fibers
Wood + Sheet metal (wavy)		Coconut fibers, cotton wool, straw bale, reed panels, wood fibers
SEB + Sheet metal (wavy)		Coconut fibers, cotton wool, straw bale, reed panels, wood fibers
Banco + Sheet metal (wavy)		Coconut fibers, cotton wool, straw bale, reed panels, wood fibers

The composition of the building elements used in the insulation process is outlined in Table 2.

The thermal properties of the materials used to construct the habitat are outlined in Table 3.

Table 3. Thermal properties of the materials used to construct the habitat [44–47].

Materials	Thermal Conductivity λ (W·m^{-1}·K^{-1})	Density ρ (Kg·m^{-3})	Heat Capacity Cp (J·Kg^{-1}·K^{-1})
Sheet metal	50	7800	450
Tile	1.73	2243	920
Straw	0.065	100	2000
Reed	0.055–0.09	120–255	1400–2000
Typha	0.03319	360	-
Banco	0.5–1.5	1600–1900	600–1000
Stone	1.4	1895	1000
Wood	0.15	1200	480
BTS	1.1	1500	2000
Breezeblock	0.833	1000	1000
Concrete	1.4	1001	2300
Terracotta	1–1.35	1700–2100	-
Granite	2.8	2600	1000
Cement plaster	1.4	2240	840

2.2. Meteorological Data

The research utilized the Lomé climatic data for a prototypical day in March, characterized by a global irradiance of 800 W/m^2 and ambient temperature ranging from a maximum of 35 °C to a minimum of 25 °C. These data enabled the authors to ascertain the variations in ambient temperature and solar flux on an hourly basis by considering the sinusoidal variation illustrated in Figure 1.
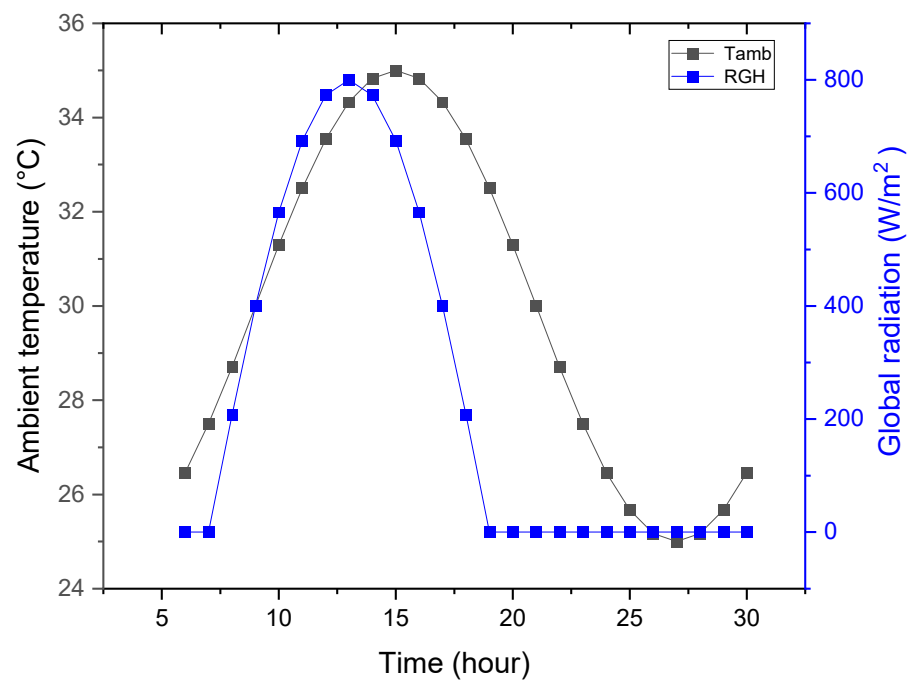
Figure 1. Mean daily sunshine and ambient temperature for a typical day in March (14 March 2024).

The numerical code was formulated utilizing the Fortran 95 language while employing the Origin software for curve plotting. As demonstrated in Figure 1, the temporal progression of both global solar radiation (R_(GH)) and ambient temperature (T_(amb)) for a standard day in March (14 March 2024), notably the hottest day of the year, is presented. The utilization of climatic data from this day as the input data for the numerical code was

deemed appropriate, as it facilitated an analysis of the thermal behavior of the building under Lomé external climatic conditions.

2.3. Method

2.3.1. Description of the Building Model

The simulated building constitutes a mono-zone of 16 m^2 of living space and 3 m in height, situated on the ground and comprising two windows and a wooden door in the southern wall. The dimensions are 1.2 × 1.4 for the windows and 1.1 × 2.1 for the door. The walls of the building are 3 m in height and 15 to 20 cm thick. They are covered with a cement plaster of 2 cm in thickness for the specific type of wall in question. The windows and door remain open between 6 a.m. and 6 p.m. Furthermore, the air renewal rate in the building is considered and described by an additional term added to the heat balance equation that governs the heat transfer in the building.

To achieve this, the roofs and external surfaces of the building were modeled. The simulations were conducted in two stages: initially without insulation materials and, subsequently, with insulation layers. The indoor air temperatures of the building were simulated and subsequently evaluated in terms of thermal comfort. Figure 2 provides a visual representation of the various modes of heat exchange within the habitable envelope.
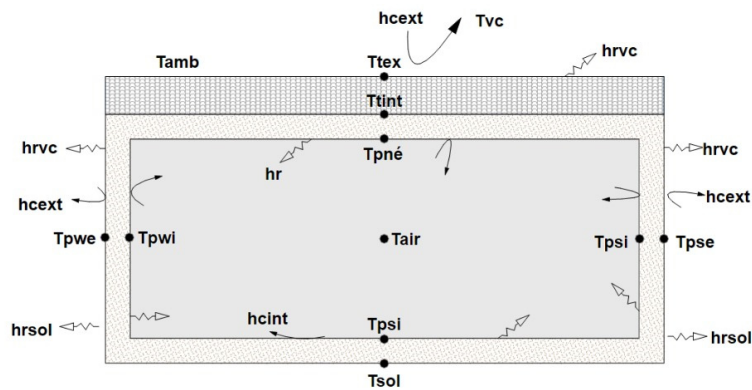
Figure 2. Descriptive diagram of the various modes of heat exchange occurring within the living building envelope.

2.3.2. Thermal Transmittance Coefficient of the Elements

In the context of heat transfer, the thermal transmittance coefficient (denoted as U) for an element can be defined as the inverse of its total thermal resistance. The total thermal resistance is a function of the thickness (d), and the thermal conductivity (λ) [47].

$$U = \frac{1}{\frac{1}{h_i} + \frac{d_1}{\lambda_1} + \frac{d_2}{\lambda_2} + \cdots + R_g + \cdots + \frac{d_n}{\lambda_n} + \frac{1}{h_i}} \quad \text{W/m}^2\cdot\text{K}$$

$$R_{total} = \frac{1}{h_i} + \frac{d_1}{\lambda_1} + \frac{d_2}{\lambda_2} + \cdots + R_g + \cdots + \frac{d_n}{\lambda_n} + \frac{1}{h_i}$$

$d_1 \ldots d_n$: Layer thickness of the corresponding material in m.
h_i, h_e: Surface heat transfer coefficient, in W·m^{-2}·K^{-1}.
$\lambda_1 \ldots \lambda_n$: Thermal conductivity of the corresponding material in W·m^{-1}·K^{-1}.
R_g: Air layer thermal resistance in m^2·K·W^{-1}.
R_{total}: Total thermal resistance of the element in m^2·K·W^{-1}.
Figure 3 illustrates the implementation of the insulation at the roof and wall level.
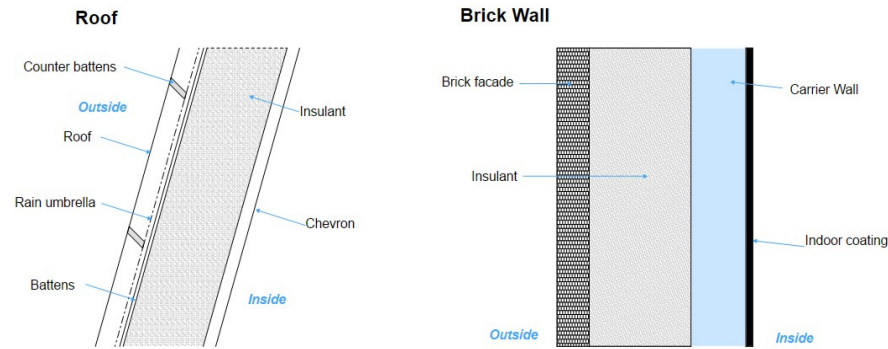
Figure 3. Diagram illustrating the implementation of the insulation in the roof and the wall.

2.3.3. Mathematical Formulation

Based on the thermal behavior of our habitat model, we have adopted a methodology based on nodal analysis, as set out in references [48,49].

2.3.4. Simplifying Assumptions of the Equation

Heat transfers occur directionally; the thermal inertia of air can be regarded as negligible; the materials can be considered to exhibit the properties of gray bodies; the rate of air renewal within the habitat enclosure is variable; the transfer fluid is assumed to be air, a perfect and incompressible gas; the thermal properties of materials are assumed to be constant and independent of temperature; and ambient temperature and sunlight act as instantaneous functions on all wall and roof surfaces.

2.3.5. Basic Energy Transfer

The formulation of transfer equations is founded upon an analogy between thermal and electrical transfers. The instantaneous variation in energy within a given component of the habitat is equal to the algebraic sum of the flux densities exchanged within said component. The aforementioned equation is presented as follows:

$$\frac{M_i C_{P_i} \partial T_i}{s \partial t} = \mathrm{DFS}A_i + \sum_{i=1}^{n} \sum_x h_{xij}(T_j - T_i) \tag{1}$$

φ_{xij} is the heat flux density exchanged by the transfer mode (conduction, convection, and radiation) between media (*i*) and (*j*) (w·m^{-2}).

s is the cross-section of the wall in (m^2).

$\mathrm{DFS}A_i$ is the density of solar flux absorbed by the material (*i*).

$$\mathrm{DFS}A_i = \alpha_i \varphi_i \tag{2}$$

α_i is the heat absorption coefficient of the material.

φ_i is the solar flux density captured by the surface of the medium (*i*) (w·m^{-2}) by introducing a h_{xij} exchange coefficient and linearizing the transfers. Thus, we can write

$$\varphi_{xij} = h_{xij}(T_j - T_i) \tag{3}$$

Thus, Equation (1) is written as follows:

$$\frac{M_i C_{P_i} \partial T_i}{s \quad \partial t} = \mathrm{DFS}A_i + \sum_{i=1}^{n} \sum_x h_{xij}(T_J - T_i) \tag{4}$$

Equation (4) is applied to the various walls and roofs of the systems studied.

Governing equations at the roof level are written as follows:

The external wall of the roof is represented by the following equation:

$$\frac{M_{tex}C_{P_{tex}}}{S}\frac{\partial T_{tex}}{\partial t} = \alpha_{tex}\varphi_{tex} + \frac{K_{tex}}{E_{p_{tex}}}\left(T_{ti} - T_{tex}\right) + h_{c_{ex}}\left(T_{air} - T_{tex}\right) + h_{r_{vc,tex}}\left(T_{vc} - T_{tex}\right) + h_{r_{sol,tex}}\left(T_{sol} - T_{tex}\right) \quad (5)$$

The internal wall of the roof is represented by the following equation:

$$\frac{M_{ti}C_{P_{ti}}}{S}\frac{\partial T_{ti}}{\partial t} = \frac{K_{ti}}{E_{p_{ti}}}\left(T_{tex} - T_{ti}\right) + h_{c_1}\left(T_{air} - T_{ti}\right) + h_{r_{ti,pni}}F_{ti,pni}\left(T_{pni} - T_{ti}\right) + h_{r_{ti,psi}}F_{ti,psi}\left(T_{psi} - T_{ti}\right)$$
$$+ h_{r_{ti,pei}}F_{ti,pei}\left(T_{pei} - T_{ti}\right) + h_{r_{ti,pwi}}F_{ti,pwi}\left(T_{pwi} - T_{ti}\right) \quad (6)$$

Governing equations are also implemented at the building level.

Once a heat balance has been established at each node associated with the transfers in the habitat model, a series of transfer equations can be formulated as follows:

The equation for the north external wall of the building is as follows:

$$\frac{M_{pnh}C_{p_{pnh}}}{S}\frac{\partial T_{pne}}{\partial t} = \alpha_{pne}\varphi_{pne} + \frac{K_{pnh}}{E_{pnh}}\left(T_{pni} - T_{pne}\right) + h_{c_{ex}}\left(T_{air} - T_{pne}\right) + h_{r_{vc,pne}}\left(T_{vc} - T_{pne}\right) + h_{r_{sol,pne}}\left(T_{sol} - T_{pne}\right) \quad (7)$$

The north internal wall of the building is represented by the following equation:

$$\frac{M_{pnh}C_{p_{pnh}}}{S}\frac{\partial T_{pni}}{\partial t} = \frac{K_{pnh}}{E_{pnh}}\left(T_{pne} - T_{pni}\right) + h_{c_{pni}}\left(T_{airh} - T_{pni}\right) + h_{r_{pni,pipl}}F_{pni,pipl}\left(T_{pipl} - T_{pni}\right) + h_{r_{pni,psi}}F_{pni,psi}\left(T_{psi} -\right.$$
$$\left. T_{pni}\right) + h_{r_{pni,pei}}F_{pni,pei}\left(T_{pei} - T_{pni}\right) + h_{r_{pni,pwi}}F_{pni,pwi}\left(T_{pwi} - T_{pni}\right) \quad (8)$$

Indoor air in the building is represented by the following equation:

$$\frac{M_{air}C_{p_{air}}}{S}\frac{\partial T_{airh}}{\partial t} = h_{c_{pni}}\left(T_{pni} - T_{airh}\right) + h_{c_{psi}}\left(T_{psi} - T_{airh}\right) + h_{c_{pei}}\left(T_{pei} - T_{airh}\right) + h_{c_{pwi}}\left(T_{pwi} - T_{airh}\right) +$$
$$h_{c_{ti}}\left(T_{ti} - T_{airh}\right) + CQ\left(T_{amb} - T_{airh}\right) \quad (9)$$

The internal wall of the building floor is represented by the following equation:

$$\frac{M_{ppl}C_{p_{ppl}}}{S}\frac{\partial T_{pipl}}{\partial t} = \frac{K_{ppl}}{E_{ppl}}\left(T_{spl} - T_{pipl}\right) + h_{c_{ppl}}\left(T_{airh} - T_{pipl}\right) + h_{r_{pipl,psi}}F_{pipl,psi}\left(T_{psi} - T_{pipl}\right) + h_{r_{pipl,pei}}F_{pipl,pei}\left(T_{pei} -\right.$$
$$\left. T_{pipl}\right) + h_{r_{pipl,pwi}}F_{pipl,pwi}\left(T_{pwi} - T_{pipl}\right) + h_{r_{pipli,pni}}F_{pipl,pni}\left(T_{pni}T_{pipl}\right) + h_{r_{pipli,ti}}F_{pipl,ti}\left(T_{ti} - T_{pipl}\right) \quad (10)$$

The south internal wall of the building is represented by the following equation:

$$\frac{M_{psh}C_{p_{psh}}}{S}\frac{\partial T_{psi}}{\partial t} = \frac{K_{psh}}{E_{psh}}\left(T_{pse} - T_{psi}\right) + h_{c_{psi}}\left(T_{airh} - T_{psi}\right) + h_{r_{psi,pni}}F_{psi,pni}\left(T_{pni} - T_{psi}\right) + h_{r_{psi,pei}}F_{psi,pei}\left(T_{pei} - T_{psi}\right) +$$
$$h_{r_{psi,pwi}}F_{psi,pwi}\left(T_{pwi} - T_{psi}\right) + h_{r_{psi,pipl}}F_{psi,pipl}\left(T_{pipl} - T_{psi}\right) \quad (11)$$

The south external wall of the habitat is represented by the following equation:

$$\frac{M_{peh}C_{p_{peh}}}{S}\frac{\partial T_{pee}}{\partial t} = \alpha_{peh}\varphi_{peh} + \frac{K_{peh}}{E_{peh}}\left(T_{pei} - T_{pee}\right) + h_{c_{ex}}\left(T_{air} - T_{pee}\right) + h_{r_{vc,pne}}\left(T_{vc} - T_{pne}\right) + h_{r_{sol,pne}}\left(T_{sol} - T_{pee}\right) \quad (12)$$

The east internal wall of the building is represented by the following equation:

$$\frac{M_{peh}C_{p_{peh}}}{S}\frac{\partial T_{pei}}{\partial t} = \frac{K_{peh}}{E_{peh}}\left(T_{pee} - T_{pei}\right) + h_{c_{pei}}\left(T_{air} - T_{pei}\right) + h_{r_{pei,pni}}F_{pei,pni}\left(T_{pni} - T_{pei}\right) + h_{r_{pei,pwi}}F_{pei,pwi}\left(T_{pwi} - T_{pei}\right) +$$
$$h_{r_{pei,psi}}F_{pei,psi}\left(T_{psi} - T_{pei}\right) + h_{r_{pei,pipl}}F_{pei,pipl}\left(T_{pipl} - T_{pei}\right) \quad (13)$$

The east external wall of the building is represented by the following equation:

$$\frac{M_{peh}C_{p_{peh}}}{S}\frac{\partial T_{pee}}{\partial t} = \alpha_{peh}\varphi_{peh} + \frac{K_{peh}}{E_{peh}}\left(T_{pei} - T_{pee}\right) + h_{c_{ex}}\left(T_{air} - T_{pee}\right) + h_{r_{vc,pne}}\left(T_{vc} - T_{pne}\right) + h_{r_{sol,pne}}\left(T_{sol} - T_{pee}\right) \quad (14)$$

The west internal wall of the building is represented by the following equation:

$$\frac{M_{pwh}C_{p_{pwh}}}{S}\frac{\partial T_{pwi}}{\partial t} = \frac{K_{pwh}}{E_{pwh}}(T_{pwe} - T_{pwi}) + h_{c_{pwi}}(T_{airh} - T_{pwi}) + h_{r_{pwi,pni}}F_{pwi,pni}(T_{pni} - T_{pwi}) + h_{r_{pwi,pei}}F_{pwi,pei}(T_{pei} - T_{pwi}) + h_{r_{pwi,psi}}F_{pwi,psi}(T_{psi} - T_{pwi}) + h_{r_{pwi,pipl}}F_{pwi,pipl}(T_{pipl} - T_{pwi})$$

(15)

The west external wall of the building is represented by the following equation:

$$\frac{M_{pwh}C_{p_{pwh}}}{S} = \alpha_{pew}\varphi_{pew} + \frac{K_{pwh}}{E_{pwh}}(T_{pwi} - T_{pwe}) + h_{c_{ex}}(T_{air} - T_{pwe}) + h_{r_{vc,pwe}}(T_{vc} - T_{pwe}) + h_{r_{sol,pwe}}(T_{sol} - T_{pwe})$$

(16)

2.3.6. Numerical Study

The following forms are observed in the algebraic equation systems that are derived by applying energy balances to the constituent components of the housing model [50]:

$$C\frac{d\,T(t)}{dt} = -\Omega \cdot T(t) + \beta \cdot \theta(t)$$

The state vector of the temperatures observed at the various time-dependent nodes is represented by $T(t)$. Similarly, the column vector of heat capacities observed at these nodes is denoted by C, and the square matrix comprising the thermal conductances is designated as Ω. The matrix coefficient for the different nodes will be designated as β, and finally, the column vector representing the inputs to the system under study is denoted by $\theta(t)$.

Equations (5) to (16) are discretized using an implicit finite difference method, based on a Taylor series expansion that transforms partial differential equations into a system of algebraic equations. The obtained algebraic equations system is solved using the iterative Gauss-Seidel method.

At the initial time point (t_0), it is hypothesized that wall components and roofs are set to the ambient temperature. Subsequently, at $t_0 + \Delta t$, a new temperature value is calculated for walls and roof components. The system of algebraic Equations (5) to (16) is solved to calculate new temperature values, which are then compared to the arbitrary value initially selected. Should the difference between the two consecutive temperatures exceed the desired accuracy, the calculated temperature values will replace the arbitrary value, and the procedure described previously will be repeated until convergence is attained. Convergence is achieved when the following criterion is met:

$$\frac{T^{t+\Delta t} - T^t}{T^{t+\Delta t}} \leq 10^{-5}$$

3. Results and Discussion

3.1. Model Validation

The present study has been designed with two principal goals: firstly, to confirm the accuracy of the proposed model through a process of validation based on a numerical investigation of the thermal comfort of a building with a comparable bioclimatic design, and secondly, to assess the effectiveness of the model in predicting the thermal comfort of users within a real-world setting.

To achieve these objectives, the authors chose to validate the model by literature data on our model based on a numerical study carried out by Camara et al. [51], which focused on the thermal comfort of users in a similar bioclimatic building. Figure 3 illustrates the evolution of the temperature profile of the external (Ttext) and internal (Ttint) walls of the roof of a bioclimatic building. The roof is considered to be a flat wall with a rectangular cross-section, the inclination of the angle is measured at 30° concerning the horizontal orientation, and a thickness of 24 cm. The wall is constructed from 8 mm aluminum

sheets and vertical walls of stabilized earth bricks, which facilitate air convection. Figure 4 demonstrates that the results obtained in the present study regarding external and internal temperatures on rooftops are consistent with those previously documented by Camara and collaborators under analogous circumstances.
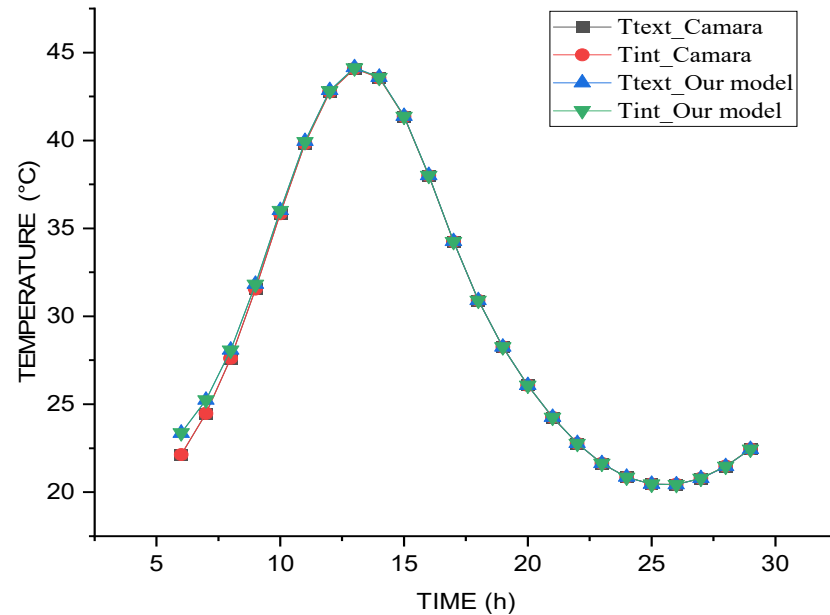
Figure 4. Model validation.

3.2. Temperature Distribution

3.2.1. Cement Block Wall Covered with Concrete Slab

Figure 5a,b shows the evolution, over time, of the temperature of the indoor air of the building (Tairh) of cement block walls covered with concrete slabs as a function of different insulating materials, respectively, for the internal insulation of the corrugated iron roof alone and the external insulation of the walls alone.

It can be seen that the reduction in the temperature of the air in the home with the thermally insulated roof vs. the non-thermally insulated roof is not significant (with a reduction from 30.8 °C to 30 °C, i.e., 0.8 °C observed for the best thermal insulant at 3 p.m.) compared to the case in which external insulation was provided by the walls alone (in which there was a reduction from 30.8 °C to 28.8 °C, i.e., from 2 °C to 2 p.m., for the best thermal insulation material, which was wood fiber). This is because, in the sub-Saharan tropics, the roof is the part of the building that is most exposed to solar radiation, which leads to an increased transmission of heat waves inside buildings. Walls receive relatively less solar radiation compared to the roof.

The use of local natural resources such as cotton fibers, coconut fibers, straw bales, reed board, and wood wool for the insulation of the roof and walls makes it possible to limit the absorption of the incident heat flux in the building and thus increase the thermal comfort of the occupants without resorting to air conditioning, which is a source of energy consumption. These results are consistent with those in the literature [52] because these bio-sourced thermal insulation local materials have lower thermal conductivity properties compared to geo-sourced insulator materials.
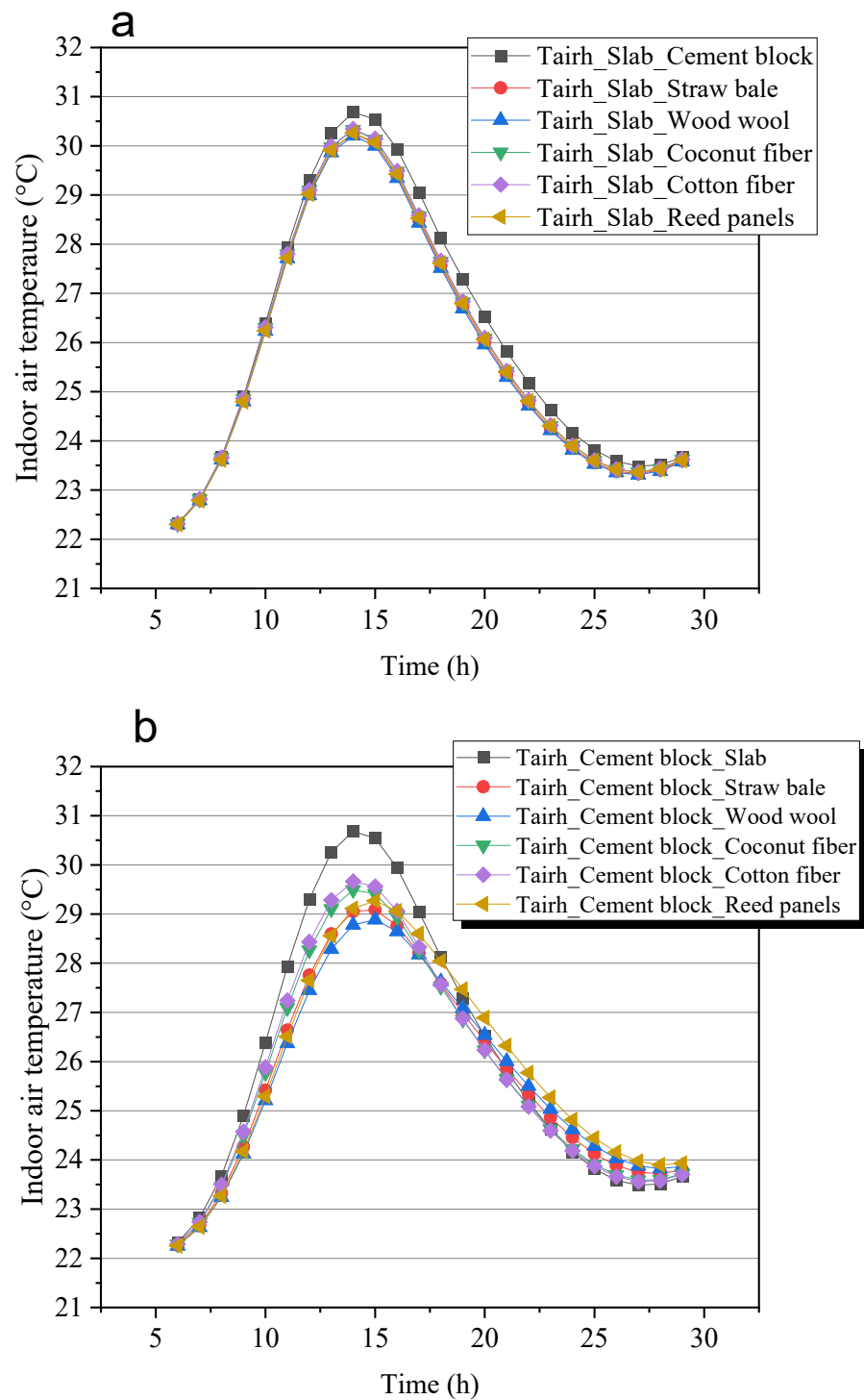
Figure 5. Variation in indoor air temperature (Tairh) of cement block wall building covered with cement concrete slabs as a function of different insulating materials, (**a**) roof; (**b**) walls.

Figure 6 shows the evolution, over time, of the temperature of the indoor air of the building (Tairh) with cement block walls covered with cement concrete slab roofs with and without insulation. In this building system, the internal insulation of the roof is coupled with the external insulation of the walls successively with cotton wool, coconut fiber, straw bale, reed board, and wood fiber. The analysis presented in Figure 6 shows that thermally insulating the roof and walls with plant-based insulation reduced the air temperature of the habitat (Tairh) by 2.6 °C, 2.7 °C, 3 °C, 3.1 °C and 3.3 °C, respectively, when coconut fibers, cotton fibers, reed board, straw bales, and wood wool were used,

compared to the uninsulated roof and walls. The addition of insulation to the underside of the cement concrete slab and the exterior face of the cement block walls seems to be an excellent solution for improving thermal comfort within this building system during hot and sunny periods [53]. These results are in agreement with those found in the literature [54]. Wood fiber, which has a low thermal conductivity value of $0.050\ \mathrm{W\cdot m^{-1}\cdot K^{-1}}$, is the most environmentally friendly insulation material available for insulating walls, roofs, or both in buildings constructed with locally eco-friendly materials.
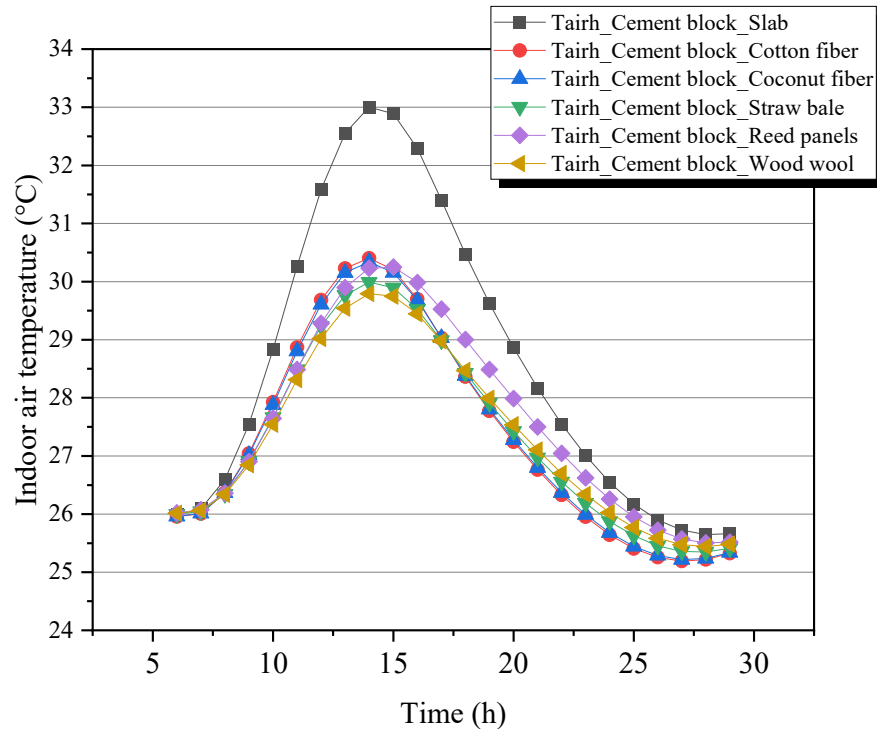
Figure 6. Variation in indoor air temperature (Tairh) of cinder block wall building covered with cement concrete slab as a function of different insulating materials, applied simultaneously to the external walls and the internal roof.

3.2.2. Stone Wall Building Covered with Sheet Metal

Figure 7a,b illustrates the evolution of the indoor air temperature of the building (Tairh) over time, showcasing the impact of different insulating materials on the temperature of the indoor air within a building with natural stone walls and sheet metal. The figures present two scenarios: the first scenario considers the internal insulation of the sheet metal roof only, while the second scenario considers the external insulation of the walls alone.

At 3 p.m., a 1 °C reduction in air temperature is observable in the domestic environment when a thermally insulating roof is in place, in comparison to a non-insulated roof, representing the optimal insulation scenario (from 30.72 °C to 29.75 °C). In comparison, the temperature reduction at 3 p.m. when external insulation is applied to the walls alone is 2 °C, from 30.8 °C to 28.8 °C, with wood fiber being the most effective thermal insulator. This phenomenon can be explained by the fact that, in tropical sub-Saharan regions, the roof is responsible for a greater transfer of heat into the built environment. In comparison to the roof, walls are exposed to a relatively lower level of solar radiation.

The analysis indicates that the roof has a higher absorptive capability than the walls when it comes to heat transfer. This phenomenon can be attributed to the discrepancy in thermophysical characteristics between these materials, namely their differing emissions. The insulating properties of stone ($1.4\ \mathrm{W\cdot m^{-1}\cdot K^{-1}}$; $1000\ \mathrm{Kg\cdot J^{-1}\cdot K^{-1}}$; $185\ \mathrm{Kg\cdot m^{-3}}$) contribute to the maintenance of a comfortable indoor temperature [52]. These out-

comes were in alignment with expectations and corroborated findings documented in the existing literature.

a

b
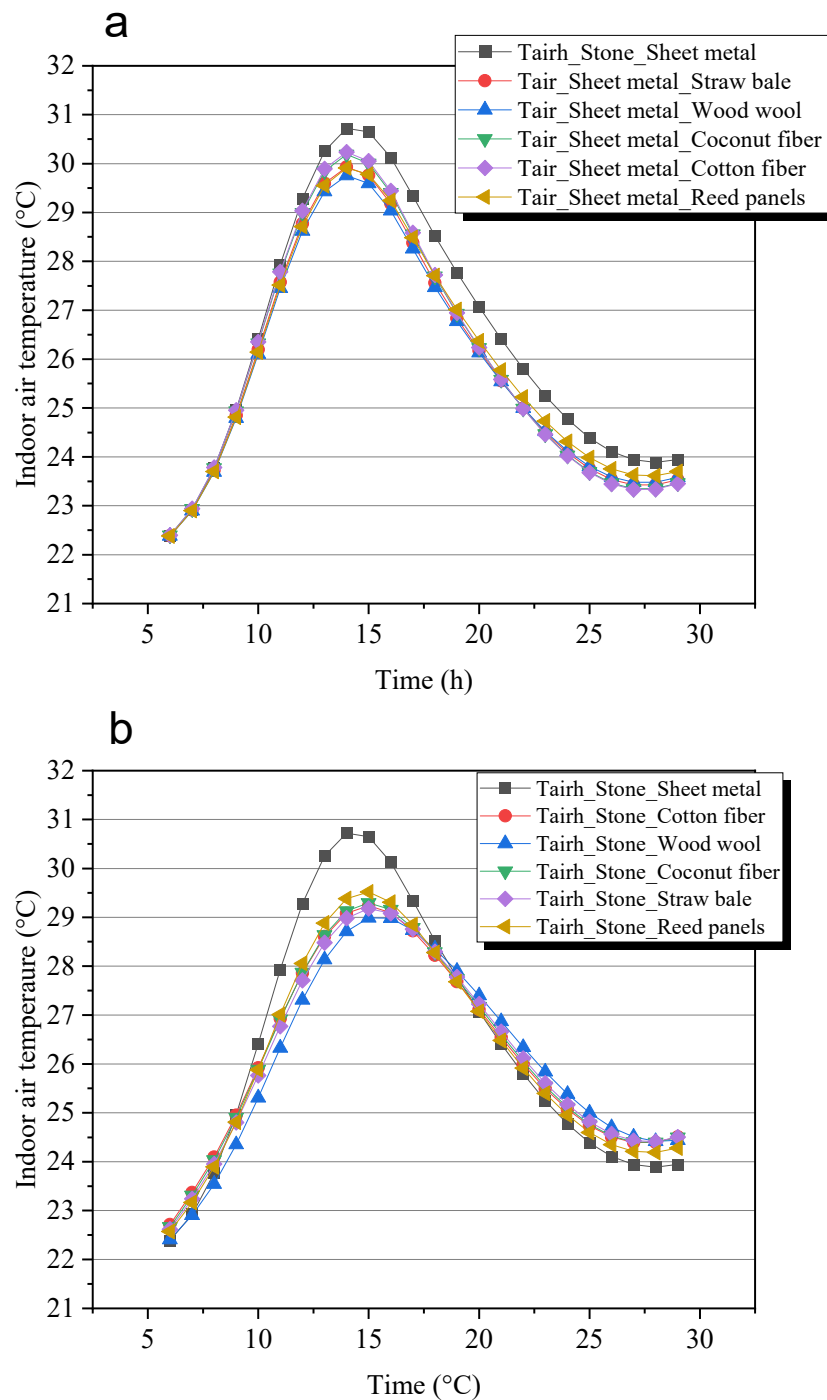
Figure 7. Indoor air temperature profile (Tairh) of natural stone wall building covered with corrugated iron roofing according to different insulating materials; (**a**) roof; (**b**) walls.

Figure 8 illustrates the evolution of the temperature of the indoor air of the building (Tairh) over time, with and without insulation, of natural stone walls topped with sheet metal roofs. In this variant, the roof insulation is coupled with external wall insulation, which is achieved successively through the use of cotton wool, coconut fiber, straw bale, reed board, and wood fiber. Figure 7 demonstrates that the implementation of plant-based insulation for the roof and walls resulted in a reduction in the air temperature of the habitat (Tairh) by up to 11% in comparison to the roof and uninsulated walls. This is

evidenced by a decrease in temperature from 32.5 °C to 29.1 °C around 2 p.m. The stone offers excellent natural insulation, which enables the maintenance of a comfortable indoor temperature and reduction in energy consumption. The construction of buildings with stone walls is environmentally friendly, as stone is a natural and durable material. The insulating properties of stone (1.4 W·m^{-1}·K^{-1}; 1000 Kg·J^{-1}·K^{-1}; 185 Kg·m^{-3}) contribute to maintaining an optimal indoor temperature throughout both winter and summer.
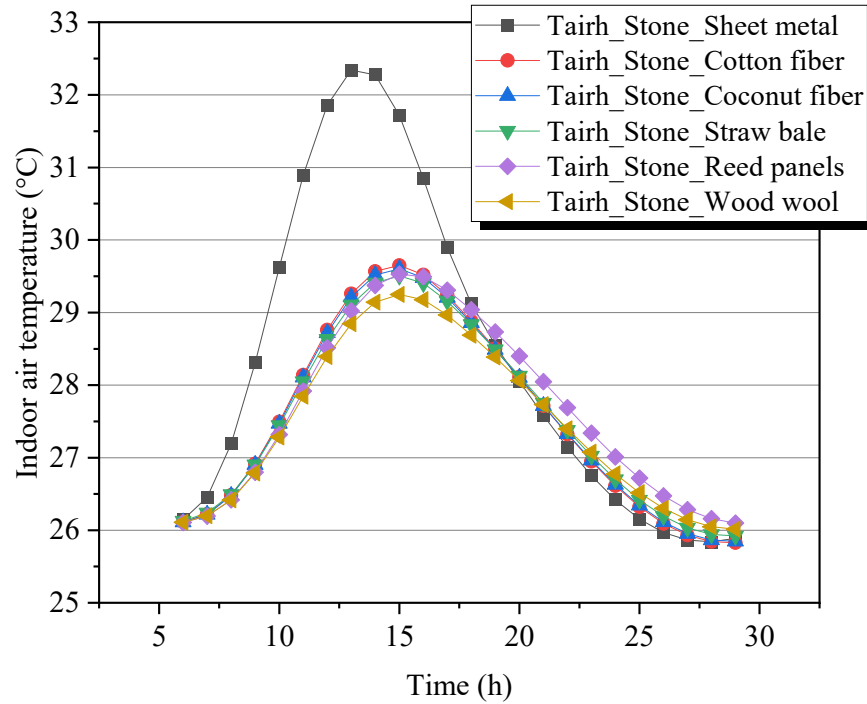
Figure 8. Indoor air temperature profile (Tairh) of natural stone wall building covered with corrugated iron roofing according to different insulating materials, applied simultaneously to the external walls and the internal roof.

3.2.3. Wooden Wall Building Covered with Sheet Metal

Figure 9a,b illustrates the temporal evolution of the indoor air temperature (Tairh) of a building with wooden walls and sheet metal roofs, as a function of different insulating materials. The figures depict the temperature reduction achieved by insulating the sheet metal roof and the walls separately, as well as the combined effect of both insulation methods.

It can be observed that at 15:00, the reduction in air temperature within the domestic environment between a thermally insulated and non-insulated roof is 0.5 °C, from 31.7 °C to 30.2 °C, for the most effective insulator. By contrast, external wall insulation alone yields an 8.2% reduction in temperature, with a drop from 31.7 °C to 29.1 °C at 2 p.m. Wood fiber represents the most effective thermal insulator in this case. This phenomenon can be ascribed to the fact that the roof plays a pivotal role in the built environment, as the primary component exposed to solar radiation. This results in a greater transmission of thermal energy within the internal environment. In comparison, the walls are exposed to a relatively lower level of solar radiation.

Thermal insulation enables the limitation of heat flow within a building, thereby enhancing the thermal comfort of its occupants without the necessity for air conditioning, which is a source of energy consumption. These findings concur with those reported in the literature [50].
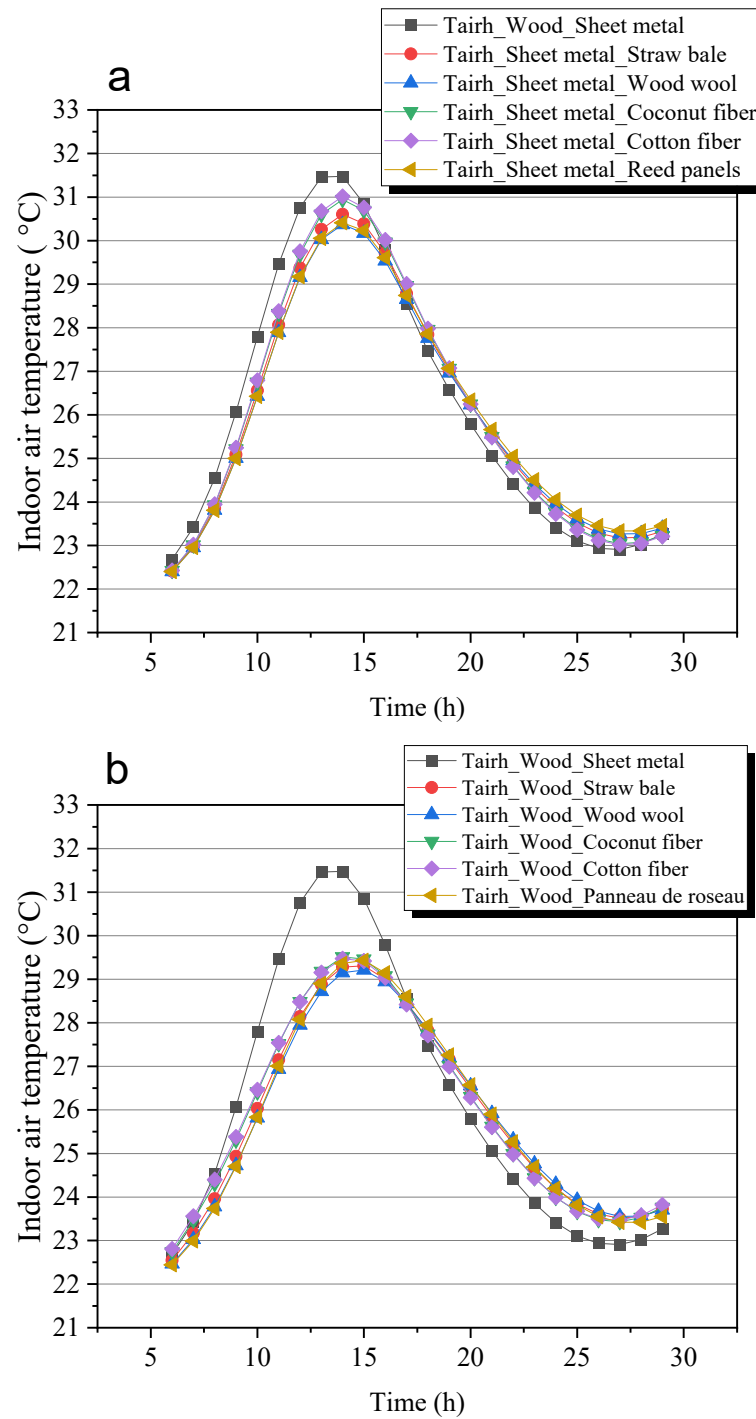
Figure 9. Indoor air temperature profile of the home (Tairh) of wooden walls building covered with sheet metal roofs according to different insulating materials; (**a**) roof, (**b**) walls.

Figure 10 depicts the evolution in temperature of the indoor air of a wooden building (Tairh) with sheet metal roofing and two different insulation types. In this construction system, the roof insulation is coupled with external wall insulation, which is achieved successively using cotton wool, coconut fiber, straw bale, reed panels, and wood fiber. As illustrated in Figure 10, applying plant-based insulation materials to the roof and walls has resulted in a notable reduction in the indoor air temperature (Tairh). This effect is particularly evident in cases where wood wool insulation has been employed, with the temperature decrease ranging from 31.9 °C to 29.4 °C. These observations highlight the efficacy of thermal insulation in reducing temperature fluctuations within a built

environment. Alternative construction materials and wooden building insulation are perceived to be more comfortable, creating a sensation of coolness and well-being. Wood is a dense material that provides effective insulation. Furthermore, wood is the sole renewable building material for long-term sustainable development.
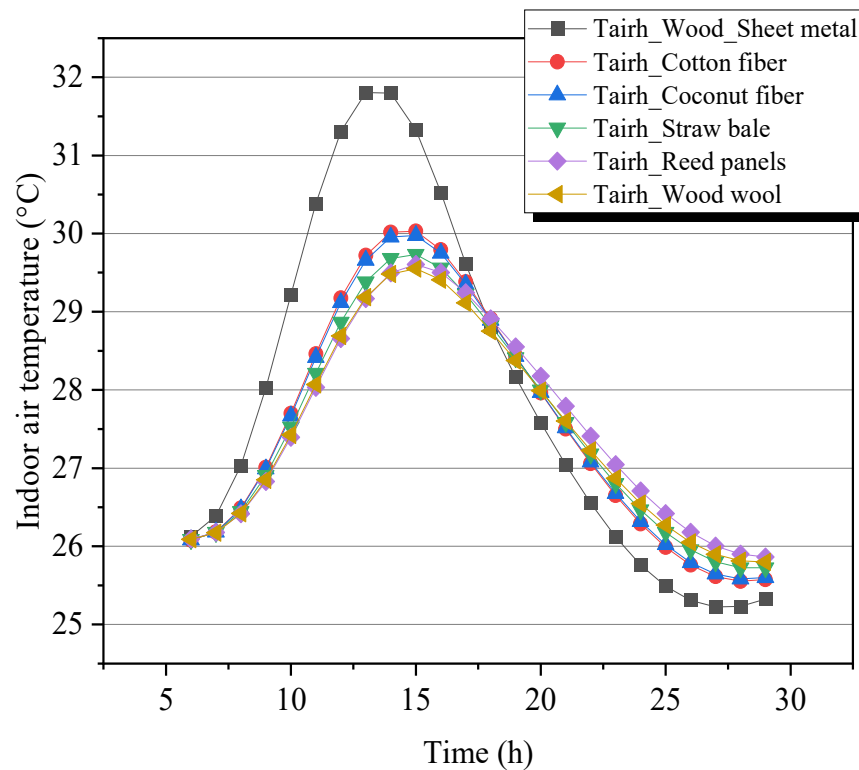
Figure 10. Variation in indoor air temperature (Tairh) of wooden wall buildings covered with cement concrete slab as a function of different insulating materials, applied simultaneously to the external walls and the internal roof.

3.2.4. Building with Stabilized Earth Brick (SEB) Walls Covered with Sheet Metal

Figure 11a,b illustrates the evolution of the indoor air temperature of the building (Tairh) for Stabilized Earth Brick (SEB) walls covered with sheet metal as a function of different insulating materials, specifically for the internal insulation of the sheet metal roof and external insulation of walls.

At 14:00, the reduction in air temperature within the building between a thermally insulated and uninsulated roof is 3.1 °C, from 32 °C to 28.9 °C, for the optimal insulation scenario. In comparison, external wall insulation permits a reduction of only 3.8 °C at 2 p.m., with a temperature drop of 31.9 °C to 27.1 °C. Wood fiber represents the most effective thermal insulator in this instance. In sub-Saharan Africa, it has been demonstrated that the roof represents the component of the building which suffers the greatest heat loss [55]. The walls typically receive a comparatively lesser quantity of solar radiation compared to the roof. Local materials, such as SEB, raw earth, and plant fibers, have been observed to exhibit superior thermal performance compared to traditional materials, including cement blocks and sheet metal [56], in the context of both dry and humid tropical climates in sub-Saharan Africa.
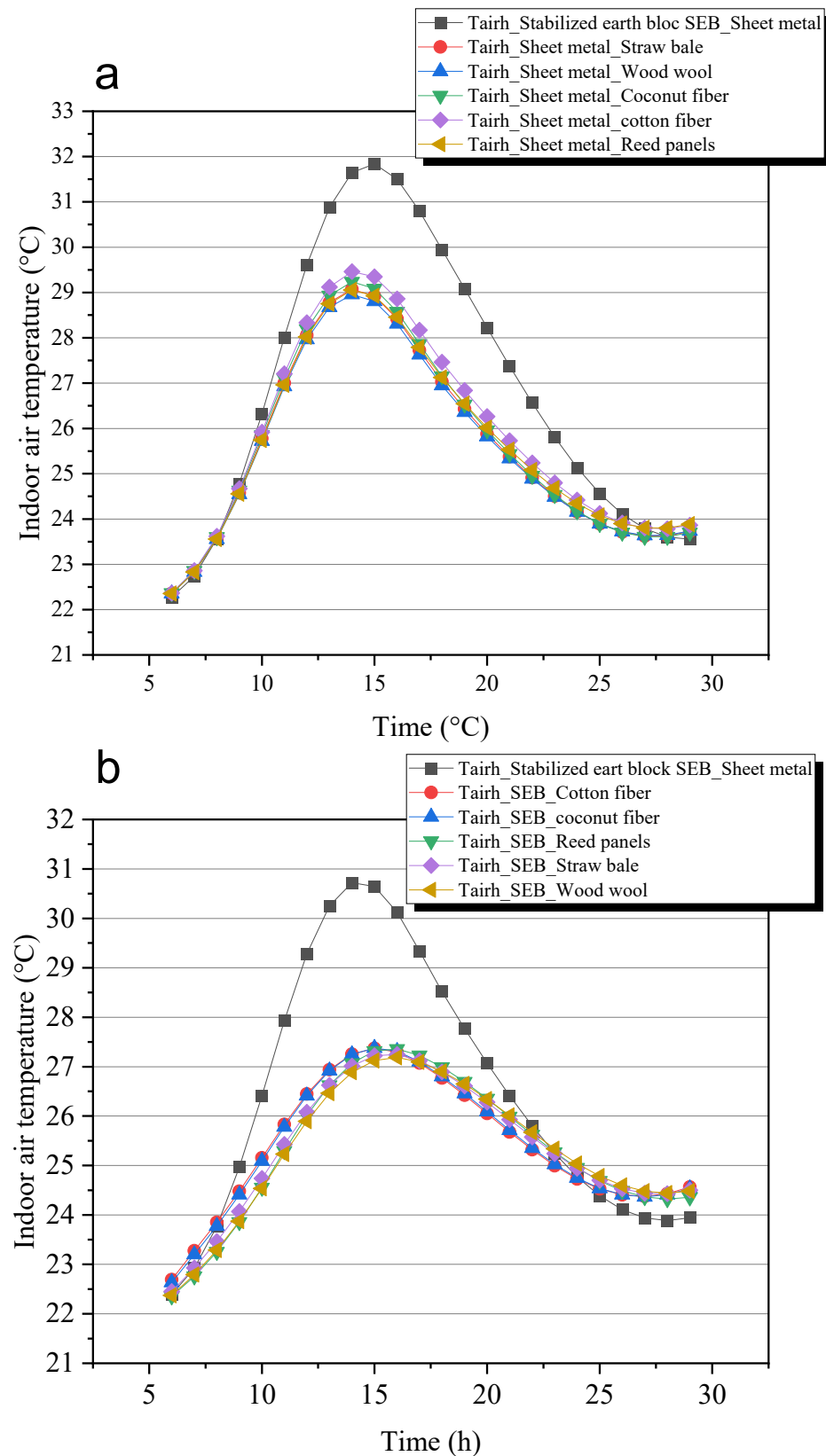
Figure 11. Variation in indoor air temperature (Tairh) of stabilized earth brick (SEB) wall building covered with sheet metal roofing as a function of different insulating materials, (**a**) roof; (**b**) walls.

Figure 12 demonstrates the evolution of the indoor air temperature of the building constructed using cement-stabilized earth blocks (SEBs), covered with metal sheet roofing, and with and without thermal insulation. The metal sheet roof and walls are insulated with

cotton wool, coconut fiber, straw bale, reed panels, and wood wool. It can be observed that the implementation of plant-based thermal insulation for the roof and walls has resulted in a reduction in the air temperature of the habitat (Tairh) by up to 12.3% in comparison with the uninsulated ceiling and walls (from 32.72 °C down to 28.7 °C). In sub-Saharan Africa, the roof is identified as the building component that experiences the highest levels of heat loss [51,54]. SEB wall buildings have high thermal inertia, resulting in a tendency to cool the interior of the building through the endothermic process of water evaporation. This explains the observed coolness of the inner wall surfaces [53,56,57].
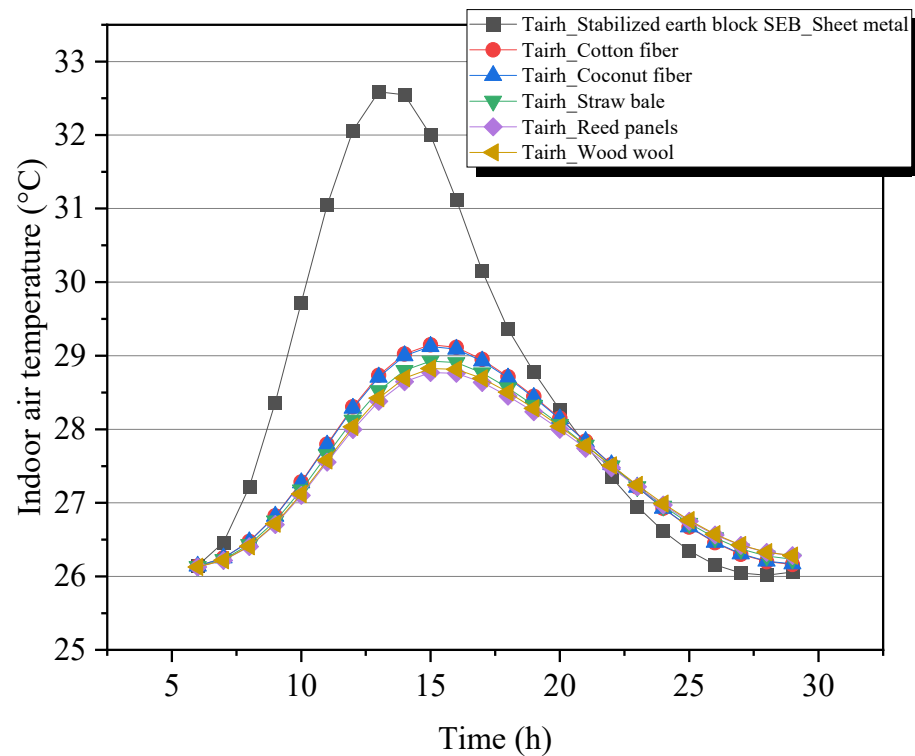
Figure 12. Variation in indoor air temperature (Tairh) of stabilized earth brick (SEB) wall building covered with sheet metal roofing as a function of different insulating materials, applied simultaneously to the external walls and the internal roof.

3.2.5. Banco Wall Building Covered with Metal Sheet

Figure 13a,b illustrates the temporal evolution of the indoor air temperature (Tairh) of a dwelling with metal sheet walls, showcasing the impact of diverse insulating materials on the internal and external insulation of the roof and walls, respectively.

A reduction of 1.5 °C in the indoor air temperature of the home was observed at 2 p.m., between a thermally insulated and uninsulated roof, with the best insulation providing a reduction from 32 °C to 30.5 °C. In comparison, the external insulation of the walls alone resulted in a reduction of 3.1 °C at 2 p.m., with a drop in temperature from 32 °C to 28.9 °C. Wood fiber is identified as the most effective thermal insulator in this context. In the context of sub-Saharan Africa, it can be observed that the roof constitutes the building component with the highest rate of heat loss, as evidenced by studies [55,58]. The utilization of local materials, such as BTS, raw earth, and plant fibers, has been observed to exhibit superior thermal performance in comparison to conventional materials [53,56,57].
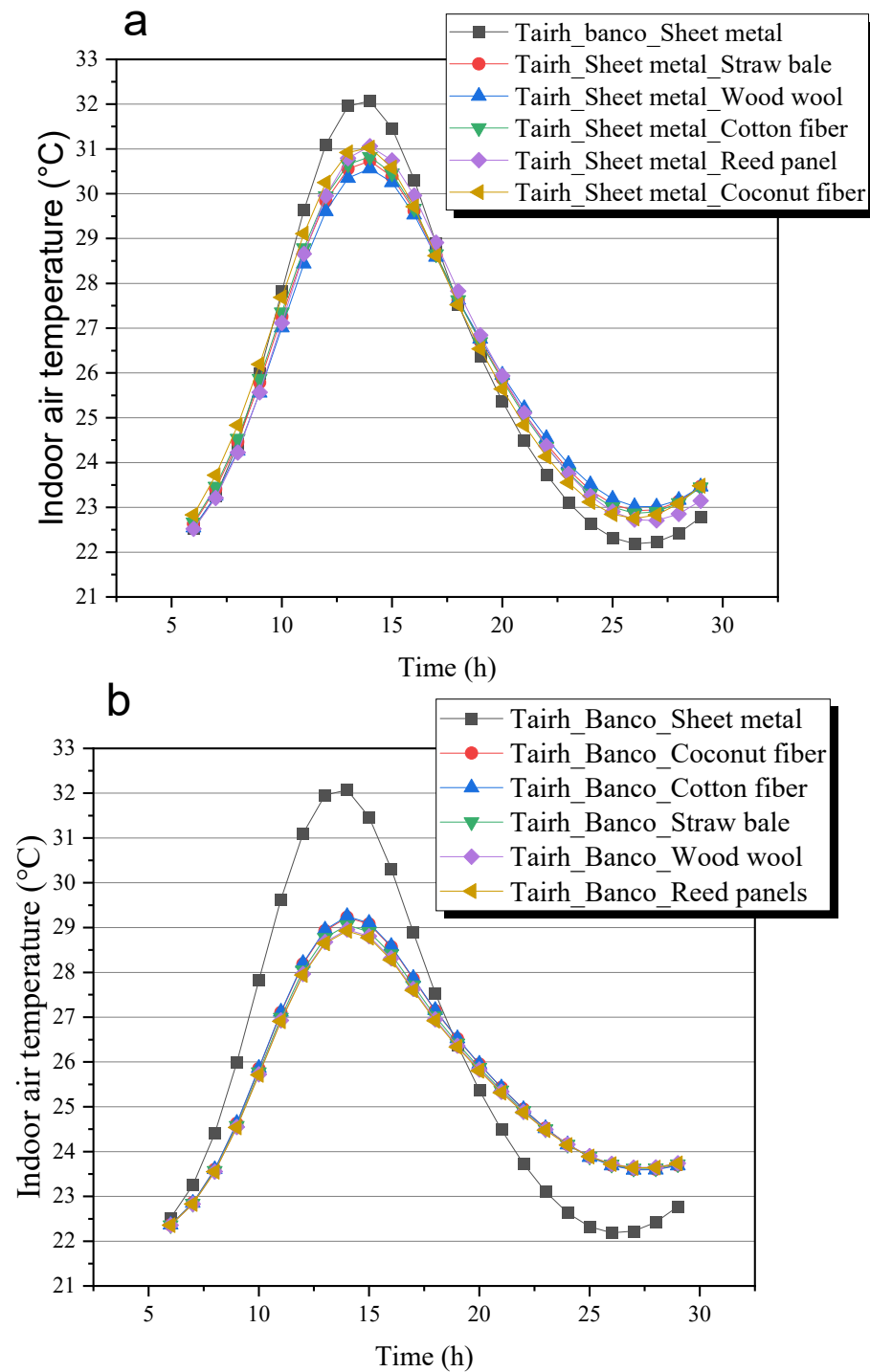
Figure 13. Variation in indoor air temperature (Tairh) of banco wall building covered with sheet metal roofing as a function of different insulating materials; (**a**) roof, (**b**) walls.

Figure 14 demonstrates the evolution of indoor air temperatures (Tairh) in the afore-mentioned building concerning the coverage of bench walls with sheet metal roofs and the presence or absence of insulation. In this construction system, the sheet metal roof and walls are thermally insulated in a series of steps, beginning with cotton wool, followed by coconut fiber, straw bale, and reed panels, and concluding with wood wool. A review of these data illustrates that roof and wall insulation using natural materials has the effect of lowering the air temperature within the building by approximately 19% in comparison to a situation where such insulation is not in place (from an average temperature of 32 °C to 26 °C). It has been demonstrated that in sub-Saharan Africa, the roof is the component of a

building with the greatest heat loss, with studies indicating this is due to a combination of factors, including poor insulation [55,58]. Banco wall buildings exhibit high thermal inertia and offer superior thermal comfort within the internal environment, both during the day and at night, compared to conventional construction materials [53,56,57].
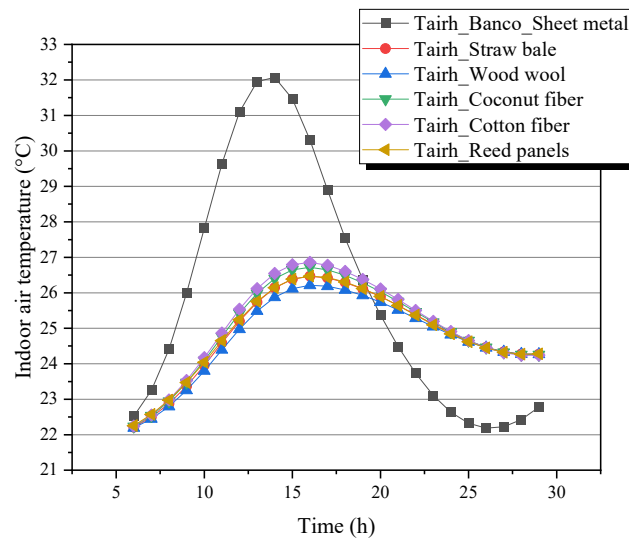
Figure 14. Evolution of the temperature profile of the indoor air of the dwelling (Tairh) of banco wall building covered with sheet metal roofs as a function of different materials, applied simultaneously to the external walls and the internal roof.

Figure 15a–e below demonstrates that wood fiber is the optimal plant fiber insulation for the simulated constructed systems. In the following section, we will examine a building with banco walls and a corrugated iron roof to investigate the impact of various parameters on thermal comfort within the structure.

(a)

Figure 15. *Cont.*

Stone Wall Building Covered with Sheet Metal

(**b**)

Wooden Wall Building Covered with Sheet Metal

(**c**)
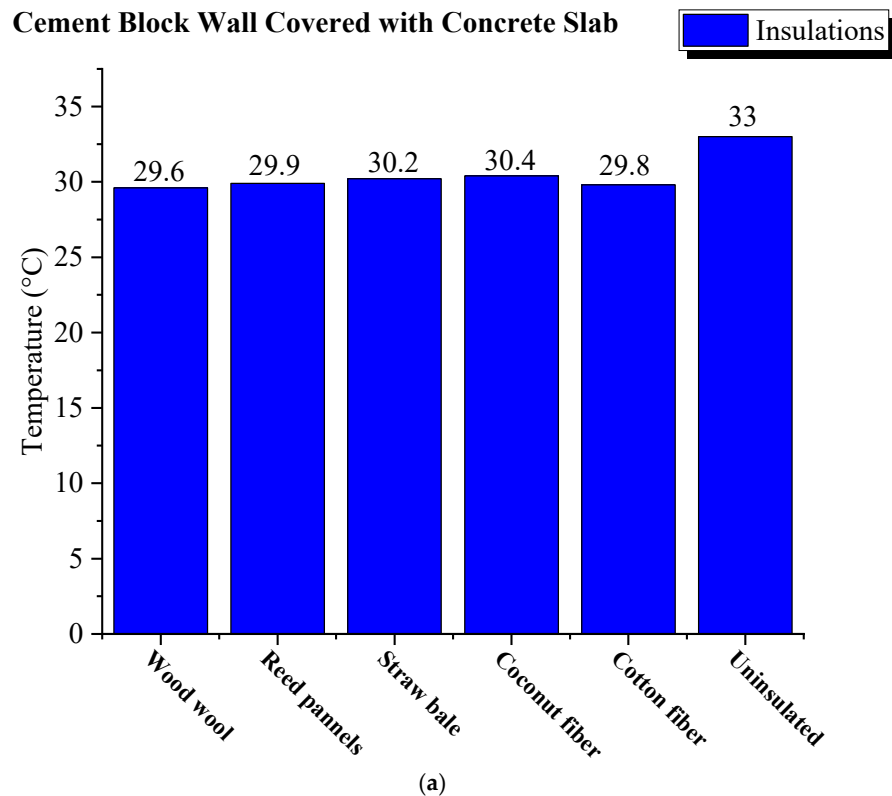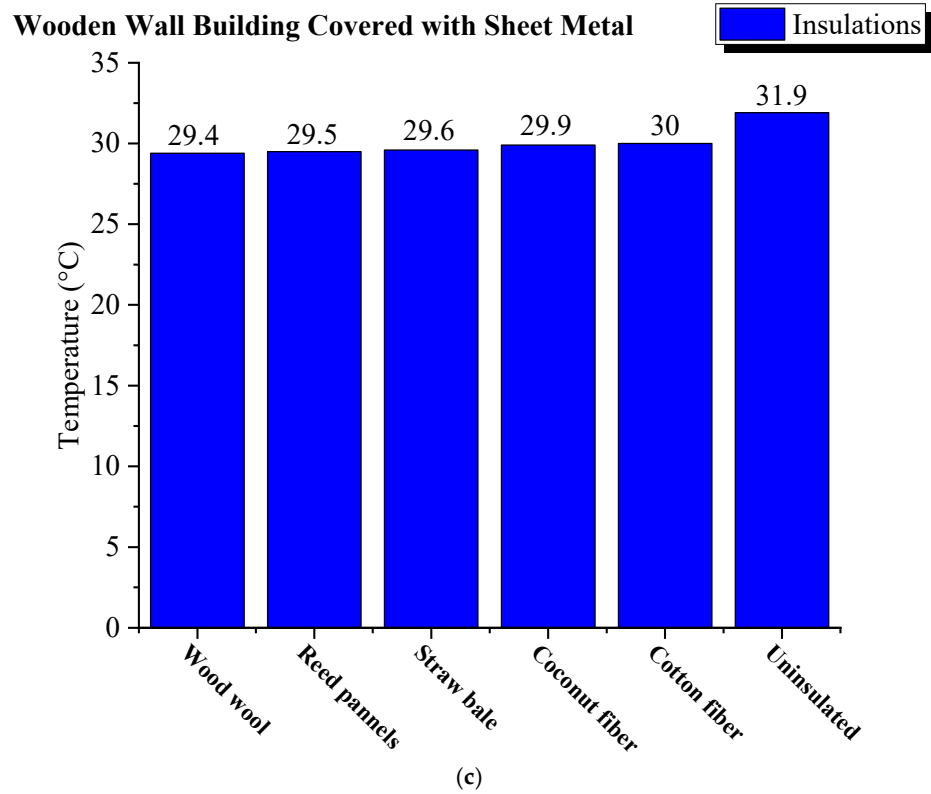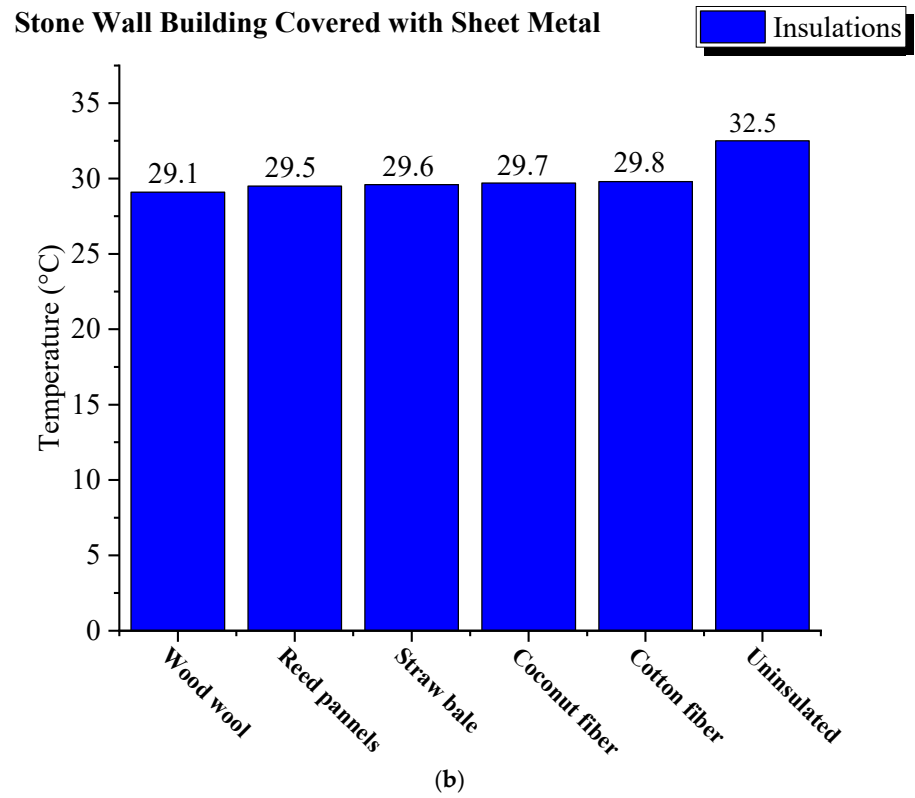
Figure 15. *Cont.*

Building with Stabilized Earth Brick walls covered with sheet metal

(**d**)

(**e**)
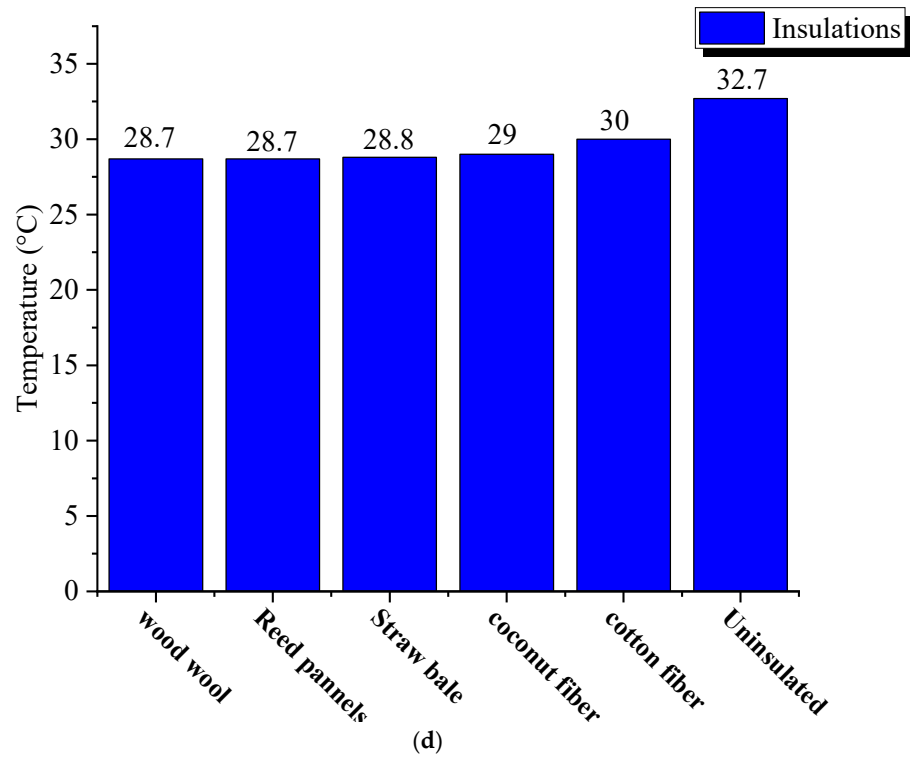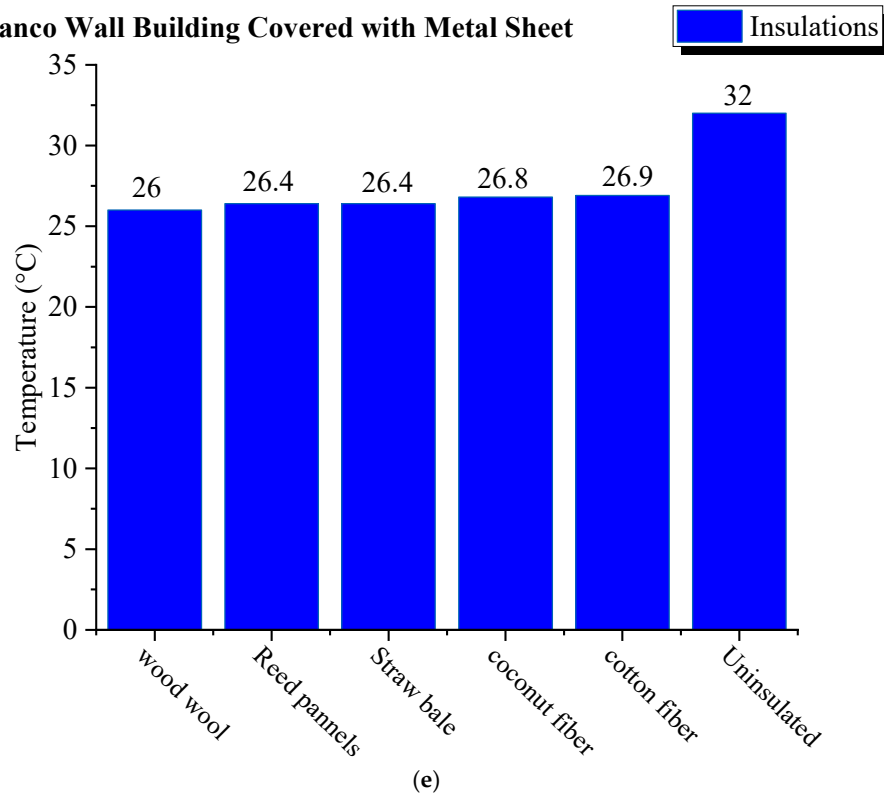
Figure 15. Comparison of indoor air temperature as a function of insulated bio-sourced materials.

3.2.6. Impact of Various Parameters on Temperature Distribution

As demonstrated in Figure 16, our investigation explores the impact of solar flux variations on the indoor air temperature of a habitat with banco walls and a corrugated metal roof, both insulated and uninsulated with 10 cm of wood fiber. An elevated solar flux in the uninsulated habitat temperature causes a rise in the indoor air temperature.

This phenomenon can be attributed to the high thermal conductivity (450 W·m^{-1}·K^{-1}) and the thin thickness (8 mm) of the metal roof, which are comparable to those observed in Sub-Saharan Africa. The majority of the heat penetrating the habitat traverses the roof. Convective heat exchange with the interior walls, which are warmer due to conductive heat transfer from the exterior walls, also contributes to air temperature inside the habitat. Conversely, the temperature within the insulated habitat increases marginally due to the enhanced thermal inertia of the walls and roof, which is attributable to the insulation. For solar fluxes of 800 W·m^{-2}, 500 W·m^{-2}, and 300 W·m^{-2}, the temperature differences between the insulated and uninsulated habitat at 2:00 p.m. are 2.7 °C, 2.6 °C, and 2.2 °C, respectively. This finding indicates that the presence of insulation serves as a temperature damper, thereby influencing the thermal environment within the habitat.
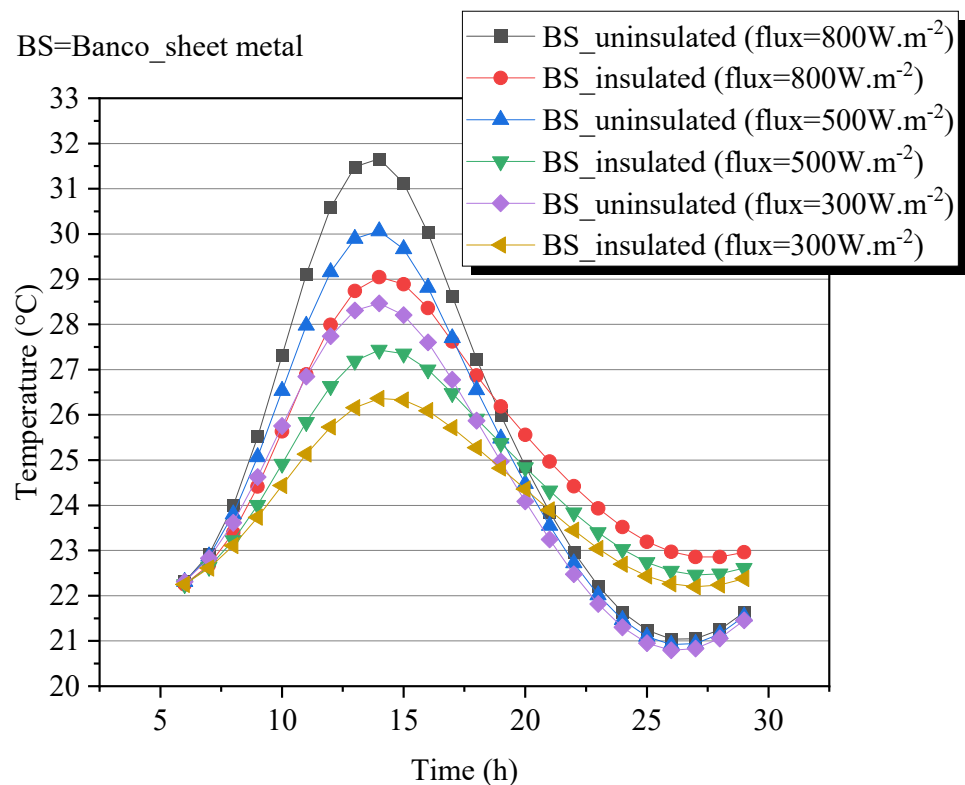
Figure 16. Influence of solar flux on air temperature inside the building.

Figure 17 illustrates the impact of maximum temperature on air temperature inside the building. This building comprises a bank wall with a corrugated iron roof and 10 cm thick wood fiber insulation. It can be observed that the curves have a similar appearance; however, it can be noted that there is an inverse relationship between the maximum temperature and air temperature inside the building. For a maximum temperature of 40 °C, the maximum temperature of the air within the residence is approximately 31.3 °C, as observed at precisely 2 p.m. At a maximum temperature of 28 °C, the indoor air temperature is 26.5 °C at 2 p.m. The ambient air impacts the thermal comfort experienced within the house.
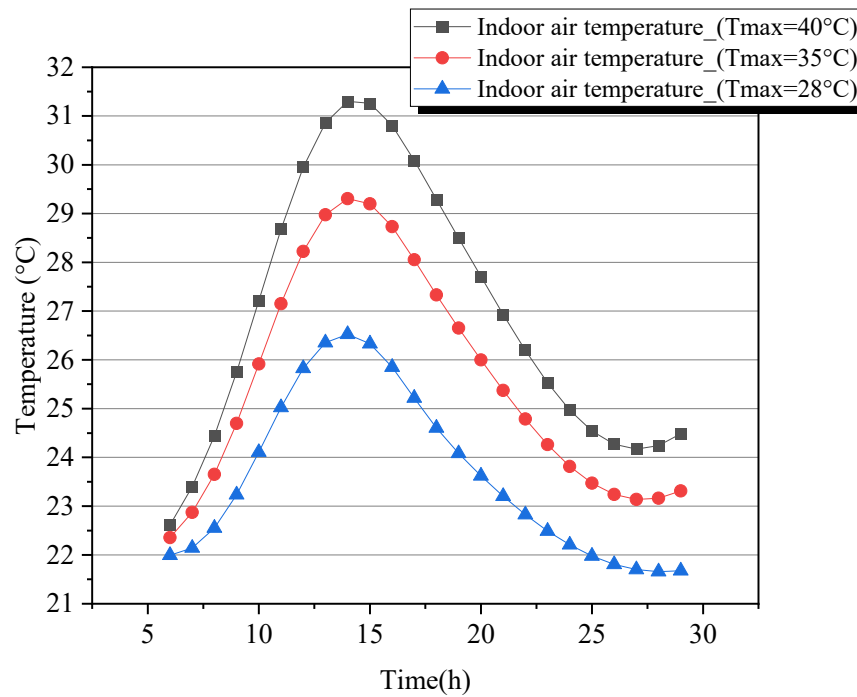
Figure 17. Influence of maximum temperature on indoor air temperature.

As illustrated in Figure 18, the indoor air temperature is significantly influenced by the minimum ambient temperature. The residential structure comprises a banco wall enclosing a roof structure comprising corrugated iron, with an insulation layer comprising wood fiber measuring 10 cm in thickness. The variation in the minimum temperature affects the temperature distribution within the domicile. For a minimum temperature of 27 °C, the maximum air temperature inside the house is observed at 2 p.m., with a recorded value of approximately 28.7 °C. If the temperature of the external environment rises due to heat transfer with the external walls of the building, this results in a higher indoor temperature being maintained for longer.
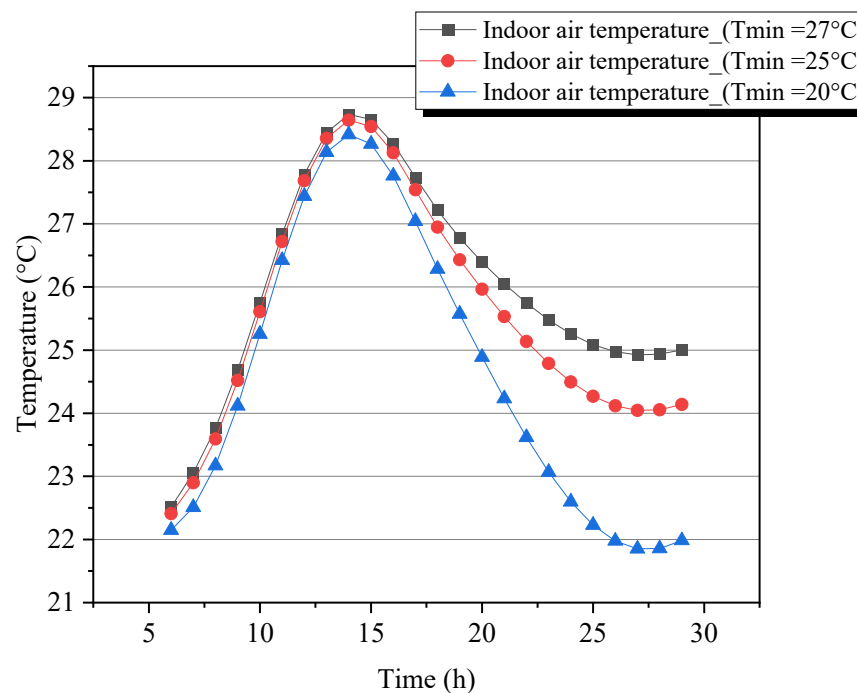
Figure 18. Influence of minimum temperature on air temperature in the house.

The impact of varying the thickness of thermal insulation applied to the walls and roof on the indoor air temperature is illustrated in Figure 19. The walls are constructed from banco and covered with metal sheet roofing, with thermal insulation provided by wood fiber. Increasing insulation thickness correlates with enhanced thermal inertia and a decreased air temperature within the dwelling. In Figure 4, the discrepancy in temperature between the various profiles remains relatively minimal in thickness. The low thermal conductivity of the material results in a minimal transfer of heat from the exterior to the interior. This, in turn, leads to the high inertia of the walls and roof.
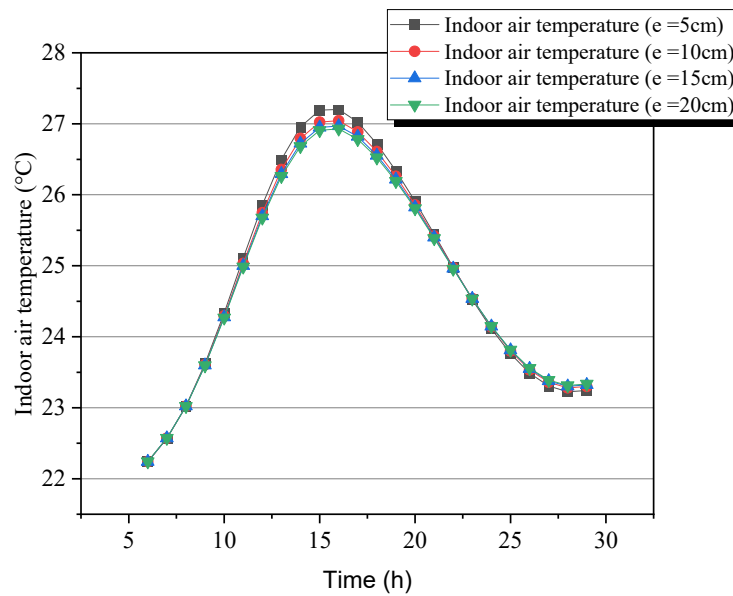
Figure 19. Influence of thickness on air temperature in the house.

3.2.7. Phase Shift and Damping of Temperature Profiles on the Walls and Roof

Figure 20 depicts the temporal evolution of the temperature profile of both the external and internal surfaces of the roof. Figure 5 illustrates that a thermal amplitude of 7 °C is recorded after a four-hour phase shift between the internal and external environments of the roof. The observed phase shift can be attributed to the thermal inertia of the system, whereas the dampening effect is predominantly attributable to the insulation applied within the roof structure.
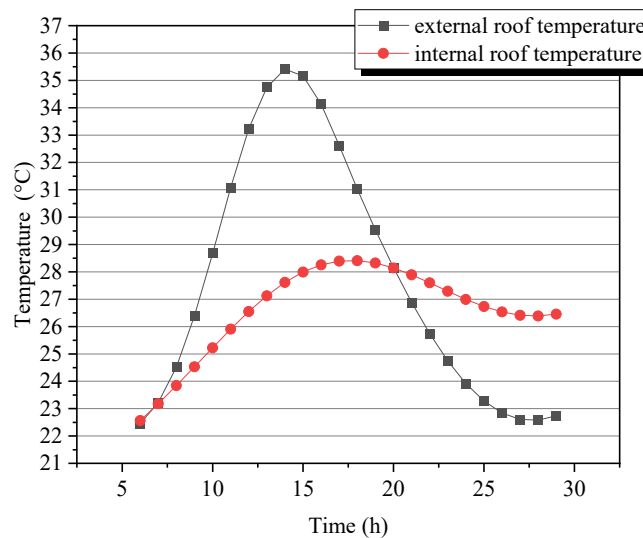
Figure 20. Temperature profile for the external and internal walls of the roof.

The evolution of the temperature profile of the wall is illustrated in Figures 21–24 for the south, north, west, and east sides, respectively. As illustrated in Figure 6, a temperature deviation of 10.3 °C is observed after a 6 h phase shift on the wall exhibiting the least exposure to solar flux during daylight hours. Figures 7 and 8 illustrate a temperature reduction of 9 °C following a 7 h phase shift. Figure 9 depicts a temperature decrease of 7.1 °C after 3 h for the wall most exposed to solar radiation over 24 h. The observed phase shifts and damping are significant, attributable to the thermal inertia resulting from absorption, the effusivity and thickness of the wall, and most notably, the impact of thermal insulation.
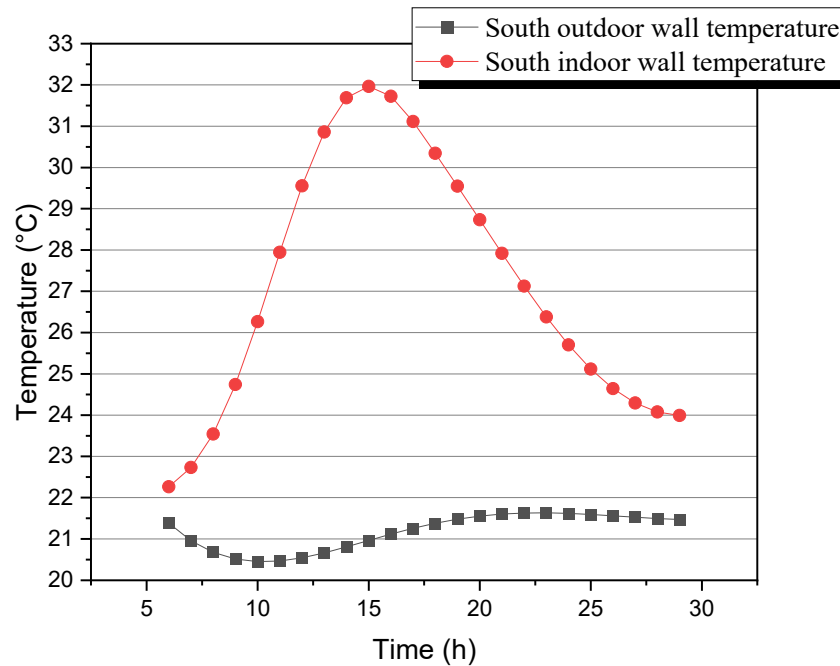
Figure 21. Temperature profile of the inside and outside of the southern wall.
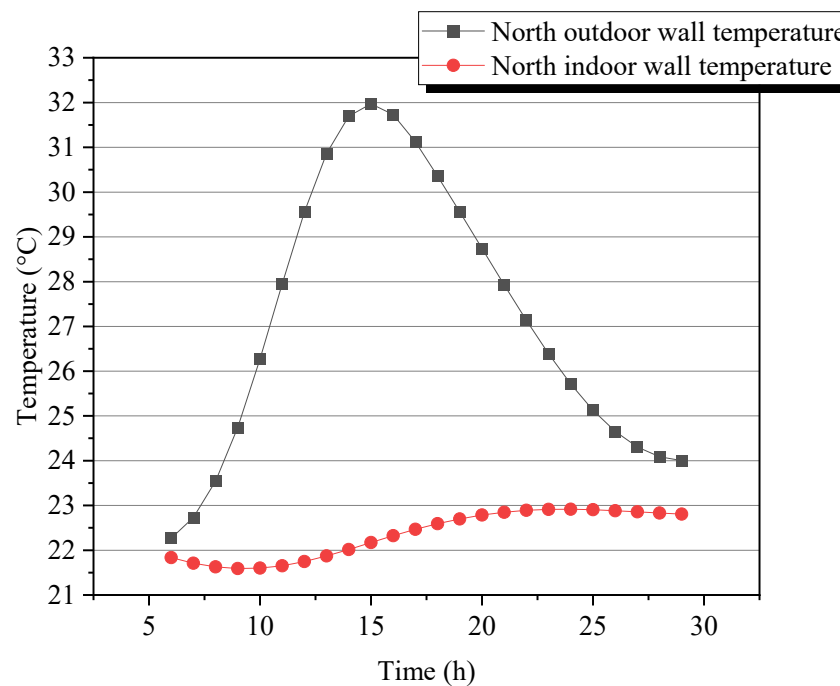
Figure 22. Temperature profile of the inside and outside of the northern wall.
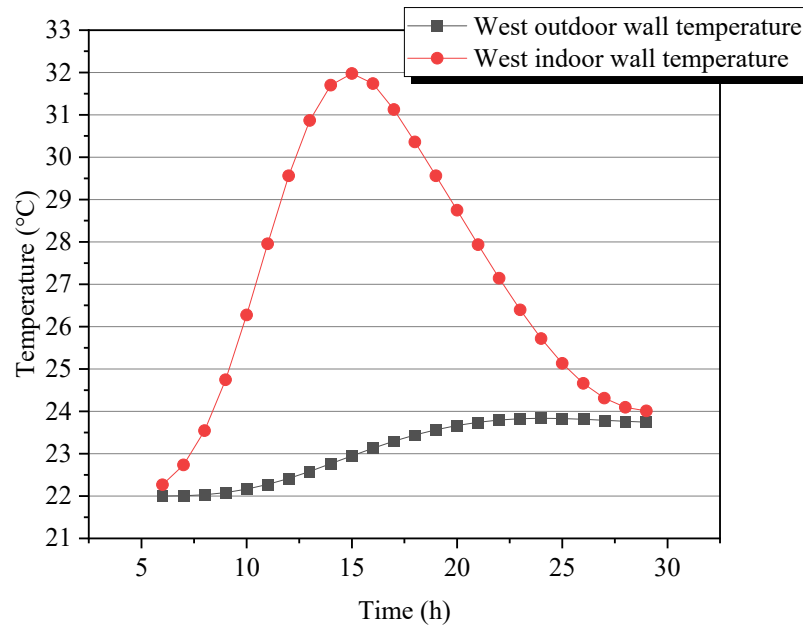
Figure 23. Temperature profile of the inside and outside of the western wall.
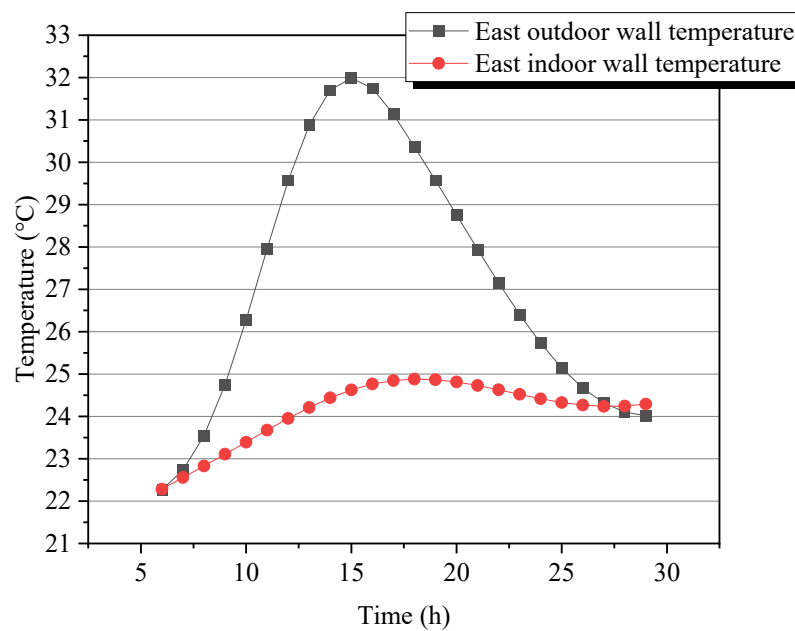
Figure 24. Temperature profile of the inside and outside of the eastern wall.

Figure 25 shows a comparative analysis of air temperatures within diverse building types, including insulated and uninsulated structures.

It is observed that the temperatures recorded in habitats made from local materials are lower than those in cement block habitats with slab roofs. Furthermore, the maximum temperature reached in the cement block structure is 29.6 °C and 33 °C. For habitats made of SEB (stabilized earth blocks) and banco, the maximum temperatures are 28.7 °C and 32.7 °C, and 26 °C and 32 °C, respectively. This can be explained by the influence of the thermophysical properties of the materials (density, specific heat, thermal conductivity, etc.). Consequently, stabilized earth blocks and raw earth offer better thermal performance compared to cement blocks' performance in tropical regions. In conclusion, we can state that local materials such as SEB and raw earth provide better comfort compared to cement blocks.
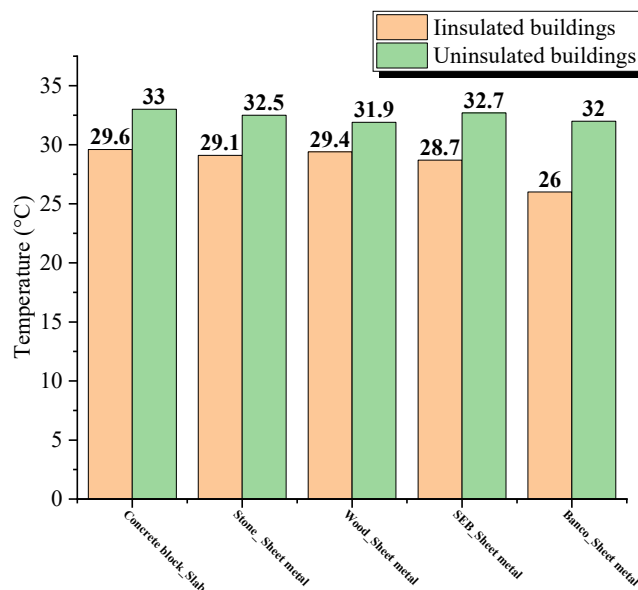
Figure 25. Comparison of air temperatures in different types of insulated and uninsulated buildings.

3.2.8. Cost–Benefit Analysis of the Local Bio-Sourced Construction Materials

The analysis of the bio-based materials mentioned, based on their thermal insulation performance, costs, and other criteria such as durability, ecological impact, and case of implementation, is summarized in detail in Table 4.

Table 4. Comparison of cost-benefit and thermal performance of insulation local materials [59,60].

Materials	Thermal Insulation Performance (λ W/m·K)	Approximative Cost (€/m²)	Advantages	Disadvantages
Wood fiber	0.036–0.045	15–30	Good thermal capacity, hygrometric regulation, durable, renewable	More expensive than other options, requires pest treatment
Cotton fiber	0.039–0.042	10–25	Lightweight, easy to handle, good acoustic insulation, recycled/recyclable	Less resistant to moisture, requires antifungal treatment
Straw bales	0.045–0.060	2–5	Very economical, excellent carbon footprint, good thermal inertia	Requires significant space (thickness), sensitive to moisture if poorly installed
Reed spannels	0.038–0.050	2–5	Moisture-resistant, biodegradable, good thermal and acoustic insulation	Requires significant space (thickness), sensitive to moisture if poorly installed
Coconut fiber	0.038–0.043	15–30	Very economical, excellent carbon footprint, good thermal inertia	Requires significant space (thickness), sensitive to moisture if poorly installed

From the findings obtained, the authors propose a suitable solution in the choice of bio-sourced materials in the realization of several projects.

Thermal performance:

- Best thermal conductivity coefficient λ (low values): wood fiber, cotton fiber, and coconut fiber
- Straw bales: still effective but slightly less efficient for thermal insulation.
  Cost:
- Most economical: Straw bales, followed by cotton fiber.
- Most expensive: reed panels and wood fiber (but they offer excellent performance and durability).
  Durability and ecology:
- Low ecological impact: all materials are renewable.
- Excellent carbon footprint: wood fiber and straw bales stand out.
  Applications:
- High-end project: Reed panels and wood fiber are suitable for premium projects or those requiring refined finishes.
- Economic and ecological projects: straw bales are ideal but require proper installation to avoid issues.
  The authors make the following recommendations:
- For cost-effectiveness, cotton fiber, and straw bales are solid choices.
- For maximum durability and performance, reed panels and wood fiber are recommended.
- Coconut fiber is an interesting alternative, though often limited by cost and availability.

4. Conclusions

The present study examines the effect of eco-friendly thermal insulation materials, namely cotton wool, coconut fiber, straw bale, reed board, and wood fiber, on improving thermal comfort within a building structure. To achieve this objective, a digital investigation was conducted on an individual dwelling constructed from a variety of locally sourced building materials and thermally insulated with environmentally friendly insulation materials.

The numerical results demonstrated that incorporating plant-based insulating materials into the building envelope resulted in a notable reduction in the indoor air temperature and the house walls, with a decrease of up to 19% compared to that obtained for uninsulated walls.

During this study, the authors were able to draw the following conclusions:

- Wood fiber emerges as the most efficacious bio-sourced material for thermal insulation, whether utilized in isolation or in conjunction with building walls and roofs.
- Construction systems based on local geo-sourced materials, such as Stabilized Earth Brick (SEB), raw earth, and banco, when coupled with plant fibers for insulation of walls, roofs, or building walls, have been demonstrated to offer superior thermal comfort compared to buildings constructed with conventional materials, including cement blocks, slabs, or metal roof sheets.
- The implementation of coupled insulation in roofs and walls of buildings is conducive to the provision of enhanced thermal comfort. This measure has been demonstrated to have a substantial impact on the reduction in the demand for electrical energy consumption for air conditioning. In addition, it can limit the rate of greenhouse gas emissions in conventional conditioning systems.
- The results of the simulations demonstrated that the utilization of wood fiber, reed panels, and straw bales as insulation materials led to a notable enhancement in comfort levels across all five building types, with an average increase of 17.5%.

The impact of these decreases in consumption on the utilization of electrical energy for air conditioning and greenhouse gas emissions is direct. However, the selection of insulation materials is influenced by several additional factors, including optimal thickness, cost, durability, fire protection, and moisture control. These aspects will be the focus of future research, but they are not addressed in the present analysis.

Abbreviations

hrsol	Wall-to-soil radiation transfer coefficient ($\text{W·m}^{-2}\text{·K}^{-1}$).
hrvc	Wall-to-Earth Radiation Transfer Coefficient ($\text{W·m}^{-2}\text{·K}^{-1}$).
K	Thermal conductivity ($\text{W·m}^{-1}\text{·K}^{-1}$).
hcex	Transfer coefficient by convection from the outside wall ($\text{W·m}^{-2}\text{·K}^{-1}$).
hr(i→pi)	Radiation transfer coefficient between other walls ($\text{W·m}^{-2}\text{·K}^{-1}$).
αtex	Absorption coefficient of the external covering (constant).
φtex	Heat flux density at the external wall (W·m^{-2}).
hrsol	Wall-to-soil radiation transfer coefficient ($\text{W·m}^{-2}\text{·K}^{-1}$).
hrvc	Wall to celestial crust radiation transfer coefficient ($\text{W·m}^{-2}\text{·K}^{-1}$).
hcex	Transfer coefficient by convection from the outside wall ($\text{W·m}^{-2}\text{·K}^{-1}$).
hr(i→pi)	Radiation transfer coefficient between other walls ($\text{W·m}^{-2}\text{·K}^{-1}$).
C	A column vector of thermal capacities at the various nodes.
φra	Exchange flux per air change (J·h^{-1}).
Ttex	External roof temperature (k).
Tint	Internal roof temperature (k).
Tsol	Ground temperature (k).
Ttamb	Ambient temperature (k).
Tvc	Temperature of the sky (k).
Tpni	Temperature of the internal north wall (k).
Tpne	Temperature of the external north wall (k).
Tpsi	Temperature of the internal south wall (k).
Tpse	Temperature of the external south wall (k).
Tpwi	Temperature of the internal west wall (k).
Tpwe	Temperature of the external West wall (k).
Tpei	Temperature of the internal east wall (k).
Tpee	Temperature of the external east wall (k).
Tairh	Indoor air temperature (k).
Tplf	Wood ceiling temperature (k).
Tpl	Floor temperature (k).
Q	Air flow rate (m^3/h).
C	Heat density of the air.
t	Time (s).
T(t)	The state vector of time-dependent temperatures at the various nodes.

References

1. UNEP. Buildings and Climate Change: Current Status, Challenges and Opportunities. *DG Environ. News Alert Dervice* **2007**, *71*, 1.
2. Tettey, U.Y.A.; Dodoo, A.; Gustavsson, L. Effects of different insulation materials on primary energy and CO_2 emission of a multi-storey residential building. *Energy Build.* **2014**, *82*, 369–377. [CrossRef]
3. Yao, R. (Ed.) *Design and Management of Sustainable Built Environments*; Springer: London, UK, 2013; pp. 1–432, ISBN 978-1-4471-4780-0. [CrossRef]
4. Philander, S.G. Fourth Assessment Report. *Encycl. Glob. Warm. Clim. Chang.* **2012**, *3*, 1–29. [CrossRef]
5. Satola, D.; Wiberg, A.H.; Singh, M.; Babu, S.; James, B.; Dixit, M.; Sharston, R.; Grynberg, Y.; Gustavsen, A. Comparative review of international approaches to net-zero buildings: Knowledge-sharing initiative to develop design strategies for greenhouse gas emissions reduction. *Energy Sustain. Dev.* **2022**, *71*, 291–306. [CrossRef]
6. Metz, B.; Meyer, L.; Bosch, P. *Climate Change 2007 Mitigation of Climate Change*; Cambridge University Press: Cambridge, UK, 2007; ISBN 978-0-521-88011-4. [CrossRef]
7. Pavel, C.C.; Blagoeva, D.T. *Competitive Landscape of the EU's Insulation Materials Industry for Energy-Efficient Buildings*; Publications Office of the European Union: Luxembourg, 2018; pp. 1–24. [CrossRef]
8. Pakdel, M.; Alemi, B. Production of Materials with High Thermal Insulation from Natural Fibers and Sericin. *Iran. J. Energy Environ.* **2022**, *13*, 314–319. [CrossRef]
9. Abedom, F.; Sakthivel, S.; Asfaw, D.; Melese, B.; Solomon, E.; Kumar, S.S. Development of Natural Fiber Hybrid Composites Using Sugarcane Bagasse and Bamboo Charcoal for Automotive Thermal Insulation Materials. *Adv. Mater. Sci. Eng.* **2021**, *2021*, 2508840. [CrossRef]
10. Veeraprabahar, J.; Mohankumar, G.; Kumar, S.S.; Sakthivel, S. Development of natural coir/jute fibers hybrid composite materials for automotive thermal insulation applications. *J. Eng. Fiber. Fabr.* **2022**, *17*, 15589250221136379. [CrossRef]
11. Vėjelis, S.; Vaitkus, S.; Skulskis, V.; Kremensas, A.; Kairytė, A. Performance Evaluation of Thermal Insulation Materials from Sheep's Wool and Hemp Fibres. *Materials* **2024**, *17*, 3339. [CrossRef]
12. Savio, L.; Pennacchio, R.; Patrucco, A.; Manni, V.; Bosia, D. Natural Fibre Insulation Materials: Use of Textile and Agri-food Waste in a Circular Economy Perspective. *Mater. Circ. Econ.* **2022**, *4*, 6. [CrossRef]
13. Schiavoni, S.; D'Alessandro, F.; Bianchi, F.; Asdrubali, F. Insulation materials for the building sector: A review and comparative analysis. *Renew. Sustain. Energy Rev.* **2016**, *62*, 988–1011. [CrossRef]
14. Raja, P.; Murugan, V.; Ravichandran, S.; Behera, L.; Mensah, R.A.; Mani, S.; Kasi, A.; Balasubramanian, K.B.N.; Sas, G.; Vahabi, H.; et al. A Review of Sustainable Bio-Based Insulation Materials for Energy-Efficient Buildings. *Macromol. Mater. Eng.* **2023**, *308*, 2300086. [CrossRef]
15. Eddib, F.; Lamrani, M.A. Effect of the thermal insulators on the thermal and energetic performance of the envelope of a house located in Marrakesh. *Alex. Eng. J.* **2019**, *58*, 937–944. [CrossRef]
16. Jie, P.; Zhang, F.; Fang, Z.; Wang, H.; Zhao, Y. Optimizing the insulation thickness of walls and roofs of existing buildings based on primary energy consumption, global cost and pollutant emissions. *Energy* **2018**, *159*, 1132–1147. [CrossRef]
17. Kaddouri, H.; Abidouche, A.; Alaoui, M.S.H.; Driouch, I.; Hamdaoui, S. Impact of Insulation using Bio-sourced Materials on the Thermal and Energy Performance of a Typical Residential Building in Morocco. *J. Adv. Res. Fluid. Mech. Therm. Sci.* **2024**, *117*, 43–59. [CrossRef]
18. Anani, A.; Jibril, Z. Role of thermal insulation in passive designs of buildings. *Sol. Wind. Technol.* **1988**, *5*, 303–313. [CrossRef]
19. Hasan, A. Optimizing insulation thickness for buildings using life cycle cost. *Appl. Energy* **1999**, *63*, 115–124. [CrossRef]
20. Cosentino, L.; Fernandes, J.; Mateus, R. A Review of Natural Bio-Based Insulation Materials. *Energies* **2023**, *16*, 4676. [CrossRef]
21. Ulutaş, A.; Balo, F.; Topal, A. Identifying the Most Efficient Natural Fibre for Common Commercial Building Insulation Materials with an Integrated PSI, MEREC, LOPCOW and MCRAT Model. *Polymers* **2023**, *15*, 1500. [CrossRef]
22. Dombaycı, A.; Atalay, Ö.; Acar, Ş.G.; Ulu, E.Y.; Ozturk, H.K. Thermoeconomic method for determination of optimum insulation thickness of external walls for the houses: Case study for Turkey. *Sustain. Energy Technol. Assess.* **2017**, *22*, 1–8. [CrossRef]
23. Kaynakli, Ö. Optimum Thermal Insulation Thicknesses and Payback Periods for Building Walls in Turkey. *Isi Bilim. Ve Tek. Dergisi-J. Therm. Sci. Technol.* **2013**, *33*, 45–55.
24. Papadopoulos, A.M. State of the art in thermal insulation materials and aims for future developments. *Energy Build.* **2005**, *37*, 77–86. [CrossRef]
25. Ozel, M. Cost analysis for optimum thicknesses and environmental impacts of different insulation materials. *Energy Build.* **2012**, *49*, 552–559. [CrossRef]
26. Nandapala, K.; Chandra, M.S.; Halwatura, R.U. A study on the feasibility of a new roof slab insulation system in tropical climatic conditions. *Energy Build.* **2020**, *208*, 109653. [CrossRef]
27. Samuel, D.G.L.; Dharmasastha, K.; Nagendra, S.M.S.; Maiya, M.P. Thermal comfort in traditional buildings composed of local and modern construction materials. *Int. J. Sustain. Built Environ.* **2017**, *6*, 463–475. [CrossRef]

28. Didier, F. *Valorisation Des Matériaux Locaux: Étude de l' Effet des Fibres de Bambou Sur Les Propriétés des BLOCS de Terre Comprimée utilisés Dans La Construction*; European University Editions: Barnet, UK, 2021.

29. Silva, C.; Chandra, M. Study on Suitable Wall Thermal Insulation Methods for Dwellings Under Tropical Climatic Conditions: A Review. 2019. Available online: https://www.researchgate.net/profile/Madujith_Chandra/publication/336614727_Study_on_suitable_wall_thermal_insulation_methods_for_dwellings_under_tropical_climatic_conditions_a_review/links/5da89511a6fdccdad54c58d4/Study-on-suitable-wall-thermal-insulatio (accessed on 2 October 2024).

30. Marín-Calvo, N.; González-Serrud, S.; James-Rivas, A. Thermal insulation material produced from recycled materials for building applications: Cellulose and rice husk-based material. *Front. Built Environ.* **2023**, *9*, 1–13. [CrossRef]

31. Zoure, A.N.; Genovese, P.V. Comparative Study of the Impact of Bio-Sourced and Recycled Insulation Materials on Energy Efficiency in Office Buildings in Burkina Faso. *Sustainability* **2023**, *15*, 1466. [CrossRef]

32. Toguyeni, D.Y.K.; Coulibaly, O.; Ouedraogo, A.; Koulidiati, J.; Dutil, Y.; Rousse, D. Study of the influence of roof insulation involving local materials on cooling loads of houses built of clay and straw. *Energy Build.* **2012**, *50*, 74–80. [CrossRef]

33. Asim, M.; Uddin, G.M.; Jamshaid, H.; Raza, A.; Tahir, Z.U.R.; Hussain, U.; Satti, A.N.; Hayat, N.; Arafat, S.M. Comparative experimental investigation of natural fibers reinforced light weight concrete as thermally efficient building materials. *J. Build. Eng.* **2020**, *31*, 101411. [CrossRef]

34. Koh, C.H.; Kraniotis, D. A review of material properties and performance of straw bale as building material. *Constr. Build. Mater.* **2020**, *259*, 120385. [CrossRef]

35. Omer, A.M. Energy, environment and sustainable development. *Renew. Sustain. Energy Rev.* **2008**, *12*, 2265–2300. [CrossRef]

36. Kemala, J.; Selamat, T.; Rusnardi, R.; Rumilla, H. Percentage of reducing heat of coco fiber material as a potential isolation of building walls. *J. Phys. Conf. Ser.* **2021**, *1811*, 012030. [CrossRef]

37. Malheiro, R.; Ansolin, A.; Guarnier, C.; Fernandes, J.; Amorim, M.T.; Silva, S.M.; Mateus, R. The potential of the reed as a regenerative building material—Characterisation of its durability, physical, and thermal performances. *Energies* **2021**, *14*, 4276. [CrossRef]

38. Sakthivel, S.; Kumar, S.S.; Mekonnen, S.; Solomon, E. Thermal and sound insulation properties of recycled cotton/polyester chemical bonded nonwovens. *J. Eng. Fiber. Fabr.* **2020**, *15*, 1558925020968819. [CrossRef]

39. Nematchoua, M.K.; Raminosoa, C.R.; Mamiharijaona, R.; René, T.; Orosa, J.A.; Elvis, W.; Meukam, P. Study of the economical and optimum thermal insulation thickness for buildings in a wet and hot tropical climate: Case of Cameroon. *Renew. Sustain. Energy Rev.* **2015**, *50*, 1192–1202. [CrossRef]

40. Daouas, N. A study on optimum insulation thickness in walls and energy savings in Tunisian buildings based on analytical calculation of cooling and heating transmission loads. *Appl. Energy* **2011**, *88*, 156–164. [CrossRef]

41. Bojić, M.L.; Loveday, D.L. The influence on building thermal behavior of the insulation/masonry distribution in a three-layered construction. *Energy Build.* **1997**, *26*, 153–157. [CrossRef]

42. Le Guide Des Matériaux Pour L' Isolation Thermique. Available online: http://doctechno.free.fr/IMG/pdf/EDF_Guide_isolation_thermique.pdf (accessed on 1 April 2024).

43. Apave; Envirobat, B.D.M. Guide Technique des Matériaux Biosourcés et Géosourcés. 2022, pp. 1–23. Available online: https://envirobatbdm.eu/sites/default/files/2022-03/2202_guide_mbs_bc_evbdm_apave_v1_0.pdf (accessed on 2 May 2024).

44. Chambre D'agriculture Franche Comte. Les Fiches Techniques: Le soja. *Recherche* 1–13. Available online: https://www.google.com/url?sa=t&source=web&rct=j&opi=89978449&url=https://bourgognefranchecomte.chambres-agriculture.fr/fileadmin/user_upload/Bourgogne-Franche-Comte/061_Inst-Bourgogne-Franche-Comte/CA71/5_Techniques_Infos/56_Grandes_cultures/soja_2022.pdf&ved=2ahUKEwjOjr-1uYuLAxXJZ_UHHR6hCfgQFnoECBcQAw&usg=AOvVaw1LaSapUMJ0tP4u8YqZ8Qpk (accessed on 2 May 2024).

45. Fohagui, F.C.V.; Koholé, Y.W.; Tchuen, G. Experimental comparison of energy performances of common types of buildings constructed in Cameroon and validation of their electrical model. *Sadhana Acad. Proc. Eng. Sci.* **2021**, *46*, 159. [CrossRef]

46. Jannot, Y.; Felix, V.; Degiovanni, A. A centered hot plate method for measurement of thermal properties of thin insulating materials. *Meas. Sci. Technol.* **2010**, *21*, 035106. [CrossRef]

47. du Bâtiment, G.L.T. Guide Les Enjeux Environnementaux De L'Isolation Thermique. *Les. Enjeux Environnementaux L'Isolation Therm.* **2015**, *143*, 143.

48. Nganya, T.; Ladevie, B.; Kemajou, A.; Mba, L. Elaboration of a bioclimatic house in the humid tropical region: Case of the town of Douala-Cameroon. *Energy Build.* **2012**, *54*, 105–110. [CrossRef]

49. Boyer, H.; Chabriat, J.; Grondin-Perez, B.; Tourrand, C.; Brau, J. Thermal Building Simulation and Computer Generation of Nodal Models. *Archit. Sci. Rev.* **2012**, *33*, 207–214. Available online: https://hal.archives-ouvertes.fr/hal-00766238 (accessed on 3 January 2024). [CrossRef]

50. Kemajou, A.; Tseuyep, A.; Egbewatt, N. Le confort thermique en climat tropical humide: Vers un réaménagement des normes ergonomiques. *Rev. Energ. Renouvelables* **2012**, *15*, 427–438. [CrossRef]

51. Camara, Y.; Chesneau, X. Étude numérique du confort thermique dans un habitat bioclimatique en brique de terre stabilisée pour un climat type de la Guinée. *Afr. Sci. Rev. Int. Sci. Technol.* **2018**, *14*, 238–254.

52. Mokhtari, A.; Brahimi, K.; Benziada, R. Architecture et confort thermique dans les zones arides Application au cas de la ville de Béchar. *Rev. Energ. Renouvelables* **2008**, *11*, 307–315. [CrossRef]

53. Robelison, S.; Lips, B. Influence thermique de l'emplacement du toit en chaume sous le toit en tôle d'un habitat à Antananarivo-Madagascar. *Afrique Sci. Rev. Int. Sci. Technol.* **2010**, *4*, 318–338. [CrossRef]

54. Bassoud, A.; Hamid, K.; Abderrahmane, M.; Abdelmalek, B. Bâtiments Construits en Adobe Salin, Durabilité Centenaire et Confort Thermique Dans un Climat Désertique. *Acad. J. Civ. Eng.* **2022**, *40*, 1–9. Available online: https://journal.augc.asso.fr/index.php/ajce/article/view/3399 (accessed on 4 November 2024).

55. Kabore, M. Enjeux de la Simulation Pour l'étude des Performances Énergétiques Des Bâtiments en Afrique Sub-Saharienne. Ph.D. Thesis, De L'université Grenoble Alpes, Saint-Martin-d'Hères, France, 2015; p. 192.

56. Dowou, K.; Nougbléga, Y.; Amou, K.A. Numerical study of thermal comfort in buildings designed with local building materials in humid tropical climate zones. *Educ. Adm. Theory Pract.* **2024**, *30*, 380–393.

57. Kemajou, A.; Mba, L. Matériaux de construction et confort thermique en zone chaude Application au cas des régions climatiques camerounaises. *Rev. Energ. Renouvelables* **2011**, *14*, 239–248. [CrossRef]

58. Fati, A.O.; Latif, B.A.; Souleymane, O.; Thierry, S.M.K.; Lewamy, M.; Joseph, B.D. The Impact of Local Materials on the Improvement of the Thermal Comfort in Building. *Curr. J. Appl. Sci. Technol.* **2020**, *39*, 22–35. [CrossRef]

59. Vignon, P. Caractérisation et Optimisation des Propriétés d' Isolants Thermiques non Tissés à Base de Fibres de Bois. Ph.D. Thesis, De L'université De Bordeaux, Saint-Martin-d'Hères, France, 2021.

60. Dickson, T.; Pavía, S. Energy performance, environmental impact and cost of a range of insulation materials. *Renew. Sustain. Energy Rev.* **2021**, *140*, 110752. [CrossRef]